Chemical Science

ROYAL SOCIETY OF CHEMISTRY

PERSPECTIVE

View Article Online
View Journal | View Issue

Cite this: *Chem. Sci.*, 2025, **16**, 19493

All publication charges for this article have been paid for by the Royal Society of Chemistry

Received 13th June 2025
Accepted 30th September 2025

DOI: 10.1039/d5sc04351d

rsc.li/chemical-science

Unveiling photoinduced electron transfers in photosensitized polyoxometalates for solar energy conversion

Christian Cariño, [a] Anna Proust, [a] Geoffroy Guillemot, [a] Ludivine K/Bidi, [a] Sébastien Blanchard, [a] Elizabeth A. Gibson [b] and Guillaume Izzet *[a]

Artificial photosynthesis faces the challenge of developing visible-light-driven strategies for converting and storing solar energy in the form of fuels and high-value chemicals. In such an approach, selective fuel production often depends on the accumulation of multiple electrons at a catalytic site. However, this process is constrained by the rapid recombination of photogenerated charges and the inherently slow kinetics of multi-electron catalytic reactions, which hinder efficient charge buildup and utilization. Polyoxometalates (POMs), a tunable class of nanoscale metal oxides, have emerged as promising multi-electron acceptors due to their redox versatility and stability. Their electron storage capabilities make them attractive as both reservoirs and catalysts. In most cases, their UV-limited absorption necessitates pairing of the POM with visible-light-absorbing antennas. Advances in photosensitized POM derivatives—via electrostatic assembly, covalent bonding, or band-gap engineering—are herein detailed. Covalent hybrids, in particular, allow precise control over electron transfer. Still, a detailed understanding of photoinduced electron transfer kinetics remains limited. This perspective article explores the potential applications of POMs in solar fuel generation, emphasizing the need for kinetic insight to design efficient, visible-light-driven photocatalysts and photoelectrochemical devices.

1 Introduction

The direct generation of chemical fuels from sunlight is a major scientific challenge for the development of a sustainable economy. To date, only few solar fuel-forming devices reaching solar-to-fuels energy conversion efficiencies exceeding the 10%

[a]*Sorbonne Université, CNRS, Institut Parisien de Chimie Moléculaire, IPCM, F-75005 Paris, France. E-mail: guillaume.izzet@sorbonne-universite.fr*

[b]*Energy Materials Laboratory, Chemistry, School of Natural and Environmental Sciences, Newcastle University, Newcastle upon Tyne, NE1 7RU, UK*

Christian Cariño

Christian Cariño is a doctoral candidate at the Insitut Parisien de Chimie Moléculaire, Sorbonne Université. He previously studied BS Chemistry in the University of the Philippines Diliman and obtained MS degree in chemistry/materials science/nanoscience through the Erasmus Mundus SERP+ program (Université Paris-Saclay/University of Genoa/University of Porto). His research interest is on (photo)electrochemical energy conversion and is currently working on photosensitizer–polyoxometalate hybrids for artificial photosynthesis under the supervision of Prof. Dr Guillaume Izzet and Prof. Anna Proust.

Anna Proust

Anna Proust has been Professor of General and Inorganic Chemistry at Université Pierre et Marie Curie, now Sorbonne Université, since 2000. She was junior member of the Institut Universitaire de France, director of the graduate school of molecular chemistry, president of the Coordination Chemistry Division of the French Chemical Society, and director of the Parisian Institute of Molecular Chemistry. In 2020, she received the State Prize of the French Academy of Sciences. Her research focuses on organometallic oxides, noble metal-substituted POMs, covalent and post-functionalization of POMs, and modified electrodes for molecular electronics and artificial photosynthesis.

range were reported.[1–10] Yet these systems mostly required the use of high-cost, low abundant materials. To efficiently perform solar-to-fuels conversion, some fundamental challenges need to be addressed, especially in charge extraction. This mostly arises from the fact that photoinduced electron transfers occur on much shorter timescales than catalysis, and so the excited carriers are lost to charge recombination (CR). Nature overcomes this problem by decoupling light-induced charge separation (CS) from catalysis, thanks to multiple reversible electronic relays.[11] Photon absorption forms single pairs of energetic electrons and holes, sequentially, while fuel-forming reactions typically require multiple electrons to be provided simultaneously by the catalyst in order to be selective for a desired product. It is therefore, desirable to accumulate charge and inhibit recombination and this is an important bottleneck in molecular photosynthesis.

In this context, polyoxometalates (POMs), a class of discrete nanosized metal oxides, are attracting attention owing to their fascinating redox properties and synthetic versatility.[12,13] As they are composed of metal ions in their highest oxidation state, they can act as multi-electron acceptors to collect, store then deliver electrons[14] to an external catalyst. Furthermore, reduced forms

Geoffroy Guillemot

Geoffroy Guillemot obtained his PhD in Chemistry in 2002 at EPFL under Prof. C. Floriani. He pursued postdoctoral research in catalysis with Prof. A. Pfaltz (University of Basel) and Dr J.-M. Basset (CPE-Lyon), then explored dioxygen activation and second coordination sphere effects with Prof. O. Reinaud (Université René Descartes) and Prof. P. Le Floch (École Polytechnique). In 2008, he joined the polyoxometalates group at IPCM, first as assistant and later associate professor in inorganic chemistry. His research focuses on designing isolated-site models based on polyoxometalates, applied to metal-catalysed atom-transfer processes and redox transformations involving coupled electron–proton transfer.

Ludivine K/Bidi

Ludivine K/Bidi graduated from Sorbonne Université, where she obtained her PhD in Molecular Chemistry in 2023 under the supervision of Dr Geoffroy Guillemot, focusing on the behavior of hybrid polyoxometalates in photo-assisted C–H activation. She then completed a postdoctoral stay with Prof. Véronique Balland at Université Paris Cité. She is now a Postdoctoral Associate in the Mayer Research Group at Yale University, where she investigates proton-coupled electron transfer (PCET) in molecular oxides.

Sébastien Blanchard

Sébastien Blanchard graduated from the Ecole Supérieure de Physique et Chimie Industrielles de la ville de Paris in 1997 and then completed his PhD in Molecular Inorganic Chemistry at University Paris Sud under the guidance of Pr. J.-J. Girerd and Dr G. Blondin. After a postdoctoral fellowship with Pr. K. Wieghardt at MPI fuer Bioanorganische Chemie, now Energie Conversion, he was appointed in 2005 assistant professor at UPMC, now Sorbonne University, and recently promoted to Professor. His research interests revolved around the bioinorganic chemistry of polyoxometalates, from their interaction with amyloid peptides to their functionalization toward bioinspired photocatalytic applications.

Elizabeth A. Gibson

Libby is Professor of Energy Materials at Newcastle University, where she has progressed from Lecturer (2014) to Reader (2018) and Professor (2022). She previously held research fellowships at Nottingham (Anne McLaren) and with the Royal Society (Dorothy Hodgkin). After completing her PhD at the University of York in 2007 under Robin Perutz FRS and Anne-Kathrin Duhme-Klair, she established a research group developing materials and devices for sustainable energy, fuels, and feedstocks. She also leads major initiatives including the Northern Net Zero Accelerator PB-IAA, the EPSRC ReNU CDT, and co-directs the EPSRC/NERC Centre "Great British Chemicals".

Guillaume Izzet

Guillaume Izzet graduated from the Ecole Nationale Supérieure de Chimie de Paris and obtained his PhD in 2004 under the supervision of Prof. O. Reinaud at Université Paris-Sud. He then pursued postdoctoral research with Prof. A. Harriman at Newcastle University and later with Prof. J. Michl at the Academy of Sciences of the Czech Republic. Appointed CNRS researcher in 2008, he is now research director at Sorbonne Université, and co-leads the e-POM group with Prof. A. Proust. His research focuses on inorganic supramolecular chemistry, polyoxometalate functionalization, artificial photosynthesis, and molecular electronics and photonics.

of POMs also may have appealing reactivity[15–18] notably for the hydrogen evolution reaction (HER) and the reductive activation of molecular oxygen (ORR).[19] Consequently, POMs can be integrated in artificial photosynthetic devices having dual role of electron storage site and catalyst. Finally, POMs also have excellent intrinsic photocatalytic properties,[20] that is yet often limited to the UV part of the solar spectrum.[21] As a consequence their implementation into artificial photosynthetic devices often requires their prior association with a visible-range antenna. This has been achieved either by electrostatic interaction with a cationic photosensitizer[22] or by direct functionalization of the POM framework.[23,24]

Organic–inorganic POM-based hybrids, hereafter named hybrid POMs,[25–31] represent versatile models for artificial photosynthesis, although not without challenges. So far there are only few existing reports of charge photoaccumulation in hybrid POMs. Furthermore, despite numerous reports on the photosensitization of POMs, limited quantitative information on the kinetics of photo-induced electron transfers (separation, accumulation, recombination) are available, while these are of high importance in order to correlate the timescale of the photophysical processes with that of catalysis. Indeed, a challenging key-step in the use of POMs for photocatalysis is ensuring the efficient closure of the photocatalytic cycle, specifically the rate-limiting re-oxidation of the reduced POM. It is thus important to rationalize the kinetics of photoinduced electron transfer with POMs, and take into account the driving force dependence which is rarely estimated or even considered.

This perspective article will hence describe the opportunities and challenges in the use of POM derivatives as multi-electron acceptors for solar energy conversion, especially for reductive fuel formation with a particular focus on the critical role of the kinetics of electron transfer in facilitating these processes. While several transition-metal substituted POMs have been reported to display remarkable activity in the oxygen evolution reaction (OER) by water oxidation,[16] this aspect will not be covered. The photocatalytic properties of POMs in the UV region are also not considered, since we are looking towards applications in solar-driven chemistry.

2 Chemical design & electronic properties of visible range photoactive POM-based systems

A major aspect of POM chemistry stems from the wide structural and compositional diversity of these oxo-clusters associated with various synthetic routes for their functionalization. The general approach to functionalization involves the introduction of lacunae in the pristine POM framework and then occupying these sites with transition metals (referred to as transition metal-substituted POMs or TMS-POMs) or organic moieties. Although the synthetic methods for POM functionalization are beyond the scope of this perspective article, one can distinguish three types of POM-based systems able to achieve the visible-light-driven photoreduction of the POM from literature: (i) multimolecular POM–photosensitizer (PS) assemblies (especially through electrostatic interactions), (ii) covalently bound POM–PS, (iii) low band-gap POM derivatives.

2.1. Multimolecular POM/PS assemblies

The association of a POM with a cationic visible-range antenna through electrostatic interactions is a very straightforward route, that *a priori* can be implemented to all types of POMs. The evaluation of the photophysical properties of the resulting POM–PS system is however more complex as the electron-transfer quenching of the PS excited state is both dynamic and static in nature.

Among the different chromophores, the most commonly used were Ru(II)-polypyridyl complexes, following pioneering works of Balzani and coll. with Keggin-type polyoxotungstates ($[SiW_{11}O_{39}Co(H_2O)]^{6-}$ and $[PW_{11}O_{39}Mn(H_2O)]^{6-}$).[32] The association of these chromophores with Wells–Dawson-type POMs (*e.g.* $[S_2Mo_{18}O_{62}]^{4-}$ and $[S_2W_{18}O_{62}]^{4-}$) was then further thoroughly studied by the groups of Keyes and Bond.[33–35] Other polypyridyl complexes have been used, notably a cyclometalated Ir(III) complex applied to photoreduce multinuclear nickel substituted POMs in the presence of sacrificial electron donors (SEDs) to produce hydrogen.[36,37] More recently Ishitani and coll. used a tetranuclear ring-shaped Re(I) complex that formed very strong 1 : 1 adducts with Keggin-type $[XW_{12}O_{40}]^{4-}$ (X = Si and Ge) owing to the full charge compensation of the POM.[29]

Cationic porphyrins have also been applied for the photosensitization of POMs particularly by Fukuzumi and coll. and Ruhlmann and coll. who respectively used Keggin-[38] and Wells–Dawson-type POMs.[39] In the case of a monocationic porphyrin 1 : 1 POM–porphyrins complexes were observed with rather important association constant (7.5×10^2 M^{-1}).[38] When using tetracationic porphyrin and highly charged tetracobalt-substituted POMs, the formation of a 1 : 4 POM : porphyrin complex was reported with very high association constant (estimated to be 7×10^{30} M^{-4}). Although slightly counter intuitive, the photosensitization of Keggin- and Wells–Dawson-type POMs was also achieved by an anionic electron rich $[Mo_6I_8Cl_6]^{2-}$ cluster despite both species being negatively charged.[40,41]

The electrostatic photosensitization of POMs can also be achieved by incorporating POMs into photoactive MOFs, and form photocatalytic materials with high activity in reduction (HER, CO_2 reduction)[42–44] or oxidation (OER). Quantum dots-sensitized photocathodes were also associated with a tetranickel substituted POM, as HER catalyst.[45] Finally positively charged carbon dots were associated with POMs and the resulting materials showed some activity in the photoreduction of silver ions.[46]

2.2. Covalently bound POM–PS

A richness in the chemistry of POMs is the possibility to functionalize some of them by the formation of a covalent bond between the POM framework and an organic counterpart. Despite being synthetically more challenging the covalent grafting of molecular photosensitizer to POMs allows a better control of distance and stoichiometry of both redox partners.

Consequently, a more straightforward evaluation of the kinetics of photoinduced electron transfer between the excited chromophore and the POM can be determined compared to multimolecular POM/PS assemblies in which the luminescence quenching could follow different mechanisms. For this reason, Section 3 will mostly focus on the evaluation of the kinetic parameters of photoinduced electron transfers in covalently bound hybrid POM–PS systems that is at the core of this perspective. The different approaches to the organic functionalization of POMs have been extensively reviewed elsewhere.[23,24,47] Whereas the electrostatic approach can be implemented to all types of POMs, the disadvantage of covalent attachment is its applicability to limited number of POMs. Consequently, fewer variety of POM-based platforms are available. For the purposes of this perspective article, the hybrid POMs described below will only reflect the most common structural archetypes currently reported in the literature.[23,24] A selection of different covalent POM–PS hybrids relevant to the scope of this article and further discussed in Section 3 is presented in Fig. 1.

Early developments in the photosensitization of POMs include the coordination between a pyridyl-functionalized hybrid POM and Ru(II) porphyrin photosensitizer,[56] or between a TMS-POM and a photosensitizer containing a pyridyl ligand.[48] This straightforward strategy has nevertheless rather similar drawbacks as the electrostatic approach, since dissociation between the POM and the PS may occur in diluted solutions, which makes the photophysical analysis complex. Following the coordination bond approach, Yamaguchi, Suzuki and coll. reported the synthesis of a new type of stable capsule-like hybrids that could be achieved by the straightforward reaction between a trivacant lacunary phosphomolybdate $[A\text{-}\alpha\text{-}PMo_9O_{34}]^{9-}$ with organic moieties displaying pyridyl ligands.[57] Stable dimers and tetramers could be selectively synthesized by reaction with ditopic and tetratopic ligands (*i.e.* porphyrin). Such strategy was recently followed by the group of Ritchie that inserted in the capsule diarylethene pyridyl units.[55]

The group of Bonchio was among the first ones to covalently graft a visible range antenna (*i.e.* a fullerene derivative) to a lacunary decatungstosilicate through an organosilyl linker for application in organic photocatalysis.[58] The group of Peng then reported the covalent grafting of photoconductive poly(-phenylene ethynylene) onto imido functionalized hexamolybdates (*i.e.*, $[Mo_5O_{18}M{\equiv}NR]^{2-}$ and $[Mo_4O_{17}(M{\equiv}NR)_2]^{2-}$),[59,60] both using direct and post-functionalization synthetic approaches. They further used the same hybrid platforms to graft photoactive diblock copolymers.[61,62] They processed these hybrid polymers as thin film for

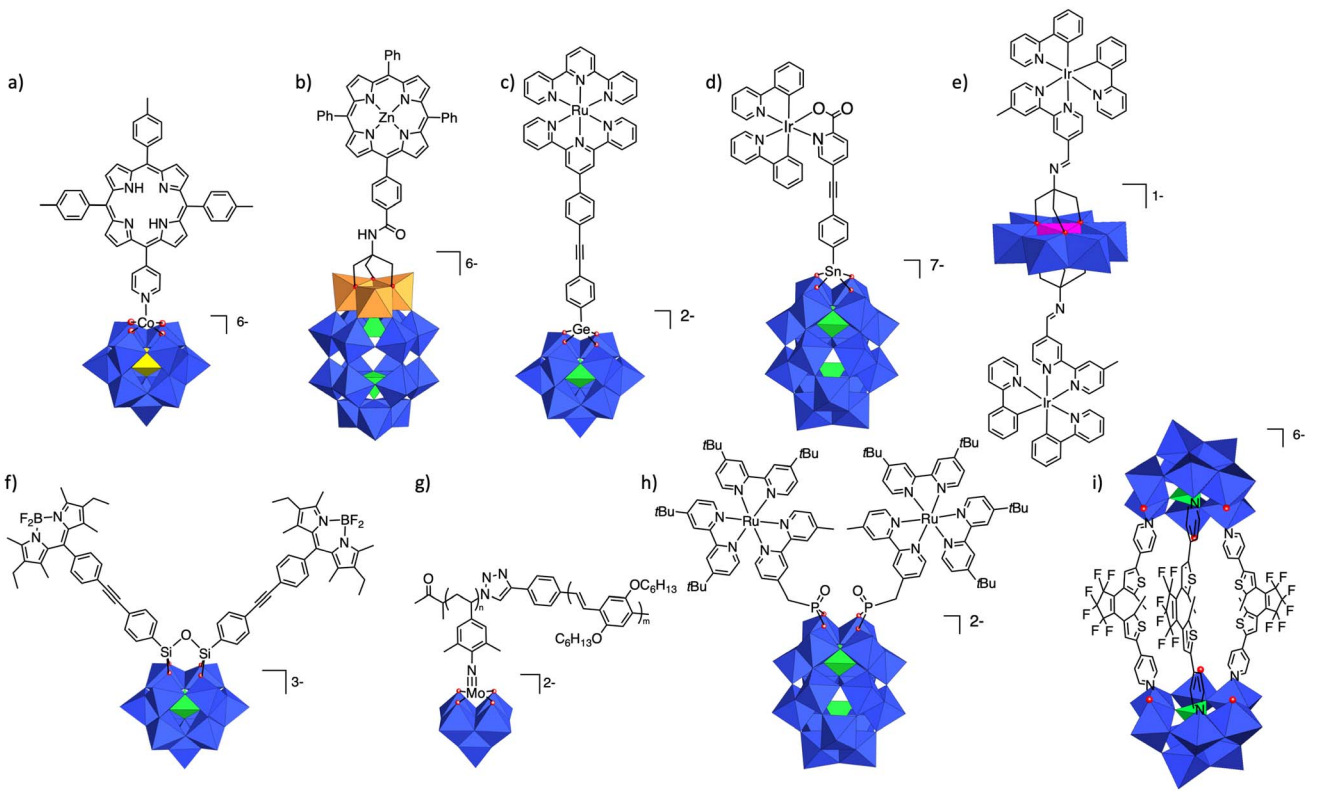

Fig. 1 Selected examples of hybrid POM–PS reported in the literature with different POM-based platforms: (a) Keggin Co(II)-porphyrin: $[SiW_{11}O_{39}Co]^{6-}$-$(C_{46}H_{35}N_5)$,[48] (b) Dawson V_3 triol-porphyrin: $[P_2W_{15}V_3O_{62}\{C_{49}H_{34}N_5OZn\}]^{6-}$,[49] (c) Keggin germane-Ru(II): $[PW_{11}O_{39}\{GeC_{44}H_{29}N_6Ru\}]^{2-}$,[50] (d) Dawson tin-Ir(III): $[P_2W_{17}O_{61}\{SnC_{36}H_{23}O_2N_3Ir\}]^{7-}$,[26,51] (e) Anderson triol-Ir(III): $[MnMo_6O_{24}\{C_{38}H_{33}IrN_5\}_2]^{-}$,[52] (f) Keggin silyl-bodipy: $[PW_{11}O_{39}\{O(SiC_{31}H_{30}N_2BF_2)_2\}]^{3-}$,[53,54] (g) imido hexamolybdate: $[Mo_6O_{18}N\{\text{diblock copolymer}\}]^{2-}$,[49] (h) Dawson phosphonate–Ru(II): $[P_2W_{17}O_{61}\{(PO)C_{48}H_{59}N_6Ru\}_2]^{2-}$,[28] (i) capsule Keggin-diarylethene: $[(PMo_9O_{31})_2\{C_{25}H_{17}F_6N_2S_2\}_3]^{6-}$.[55] Color code: blue octahedra, $\{WO_6\}$ or $\{MoO_6\}$; pink octahedra $\{MnO_6\}$, orange octahedra, $\{VO_6\}$; green tetrahedra $\{PO_4\}$, and yellow tetrahedra $\{SiO_4\}$.

photovoltaic application. Odobel, Mayer, and coll. reported then a series of hybrid POMs based on monovacant Wells–Dawson $[\alpha_2\text{-}P_2W_{17}O_{61}]^{10-}$ using organosilane and organophosphonate functionalizations. They successfully developed a post-functionalization strategy based on the Huisgen reaction with a hybrid platform displaying either azido or terminal alkyne function. In most cases, the flexible aliphatic spacer connecting the POM to the photoactive antennae (perylene mono-imide[63] and Zn(II) porphyrin[25,64]) significantly complicated the photophysical investigation owing to the presence of various conformers.

Our group further developed a series of organosilane and organotin derivatives of monovacant Keggin- and Wells–Dawson-type POMs. Through a post-functionalization approach, the POM-based platform containing one or two iodoaryl moieties were grafted to various photoactive antennae (Ru(II)[65] and Ir(III) polypyridyl/cyclometalated[31,51,66] complexes, pyrene,[65,67] bodipy,[53,54,68] porphyrins,[69,70] bis-thiophenethienothiophene[71]) using Sonogashira reactions. In this case a same PS could be grafted onto different POM-based platforms displaying distinct electron accepting properties in order to evaluate the effect of the thermodynamic parameters on the kinetics of photoinduced electron transfer (see part 2). Furthermore, rigid systems with controlled geometry could be obtained. Hasenknopf, Ruhlmann and coll. developed POM–PS hybrids using the functionalization of Anderson–Evans ($[MnMo_6O_{24}]^{9-}$), Lindqvist hexavanadate ($[V_6O_{19}]^{8-}$) and polyoxovanadotungstate Wells–Dawson ($[P_2W_{15}V_3O_{62}]^{9-}$) with triol-based ligands. Porphyrin,[49,72–74] Ru(II) complexes,[75] and Re(I)[76] complexes could then be covalently grafted onto these POM-based platforms. The Anderson–Evans platforms ($[MnMo_6O_{24}]^{9-}$, $[FeMo_6O_{24}]^{9-}$, $[CoMo_6O_{24}]^{9-}$) were also functionalized by Streb, Rau and coll. with Ir(III) cyclometalated photosensitizers[52,77] and the photophysical and photocatalytic properties of the resulting POM–Ir hybrids were thoroughly investigated by the group of Dietzek.[78–80] More recently the same consortium grafted Ru(II) tris-pyridyl complexes onto the monovacant $[\alpha_2\text{-}P_2W_{17}O_{61}]^{10-}$ through an organophosphonate functionalization.[28] Schubert and coll. also grafted Ru(II) bis-terpyridine onto a organogermane derivative of Keggin-type POM[81] using a post-functionalization synthetic route with a Sonogashira coupling reaction.[50,82,83]

2.3. Low band gap POM derivatives

Another strategy to shift the POM light absorption into the visible region is to engineer the optical gap, and in a first approximation the HOMO–LUMO gap.[84] Selected examples of low band gap POM derivatives are presented in Fig. 2. This can be achieved either through the introduction of V(V) as addenda atoms in place of W(VI) or Mo(VI), or through the use of transition metal derivatives of POMs exploiting the coordination properties of lacunary POMs, or through a combination of both approaches.[85]

The first case, corresponding to LUMO engineering, is exemplified by polyoxovanadates and mixed V/W POMs displaying LMCT from oxo-centered orbitals to the V-based

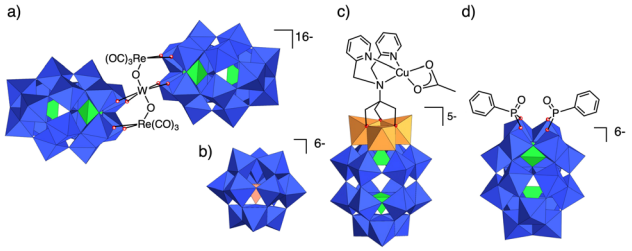

Fig. 2 Selected examples of low band gap POM derivatives. (a) $[P_4W_{35}O_{124}\{Re(CO)_3\}_2]^{16-}$,[86] (b) $[Co^{II}W_{12}O_{40}]^{6-}$,[87] (c) $[P_2W_{15}V_3O_{62}\{C_{16}H_{18}N_3Cu(C_2H_3O_2)\}]^{5-}$,[30] (d) $[P_2W_{17}O_{61}\{(PO)C_6H_5\}_2]^{6-}$,[88] color code: blue octahedra, $\{WO_6\}$; pink tetrahedron $\{CoO_4\}$, orange octahedra, $\{VO_6\}$; and green tetrahedra $\{PO_4\}$.

LUMOs tailing off in the visible range. This is the case of the bismuth capped dodecavanadates $[X\{Bi(dmso)_3\}_2V_{12}O_{33}]^-$ (X = Cl or Br) characterized by a visible absorption up to ~570 nm with enhanced extinction coefficients compared to the decavanadates ascribed to the presence of bismuth.[89]

The second category illustrates HOMO engineering and comprises mostly TMS-POMs displaying long-lived metal-to-POM charge transfer (MPCT) arising from a transition involving the inserted TM-based HOMO to purely POM-based LUMOs (Fig. 2). Pioneering examples have been given by Hill and coll. with one to three Re(I) carbonyl fragments $\{Re(CO)_3\}^+$ grafted to a monovacant $[P_2W_{17}O_{61}]^{10-}$.[86,90] These compounds are dark red and the MPCT nature of the absorption has been confirmed by computational modelling. Cobalt-containing Keggin POMs ($[SiW_{11}O_{39}Co^{II}(H_2O)]^{6-}$, $[Co^{II}W_{12}O_{40}]^{6-}$) were also investigated as these compounds displayed appealing photophysical properties.[87] Similarly, a tetranuclear Ce(III)-containing silicotungstate $[\{Ce(H_2O)\}_2\{Ce(CH_3CN)\}_2(\mu_4\text{-}O)(\gamma\text{-}SiW_{10}O_{36})_2]$ was reported to display visible light photoredox catalytic activity.[91] Many other visible-light responsive TMS-POMs have been described and used in photo-assisted catalysis but no data about the dynamics of their excited state are available.[84]

This strategy has also been applied with hybrid POMs. Our group has recently shown that the mixed V/W POM $[P_2V_3W_{15}O_{62}]^{9-}$, once functionalized with a triol-based dipyridylamine-Cu complex, could be photoexcited with visible light and was able to store successively up to 3 electrons.[30] In a series of papers, Newton, Oshio and coll. have shown that engineering the HOMO–LUMO gap of hybrid polyoxotungstates *via* the organic group allowed for visible-light sensitization of Wells–Dawson POMs.[27,88,92] Using arylphosphonate or arylarsonate functionalization, they have shown a mixing of the organic and POM orbitals both in the HOMO and the LUMO. The energy of each can be tuned by playing on the electronic properties of the substituent on the aryl ring with an increase photosensitivity to visible light with organoarsonate derivatives.[21,93]

2.4. Redox properties and absorption spectroscopy of POM–PS, coupled *versus* decoupled systems

The redox properties of hybrid POMs were reviewed in detail by Newton and coll.[94] Depending on the type of linker used to

tether the PS to the POM, two types of behaviours were observed for the resulting hybrids, depending on the electronic coupling between the POM and the organic moieties in the ground state. In the supramolecular species, following a classification proposed by Balzani,[95,96] the constituting building units are electronically decoupled and keep their intrinsic features, *i.e.* the covalent functionalization does not modify their redox properties. On the other hand, for large molecules where electronic delocalization extends across the entire molecule, it is more difficult to rationally design multi-component systems.

As regards to POM chemistry, an electron decoupling between the POM and the organic moieties is most often reported. This is the case for most Keggin and Wells–Dawson hybrid POMs, including organosilane, organotin and organogermane derivatives.[97] In these systems, density functional theory (DFT) calculations showed that the frontier molecular orbitals are either located on the organic moieties (HOMO) or the POM (LUMO, which mainly involves d_{xy} orbitals), the 14-group atom acting as a node in the molecular orbitals (Fig. 3).[51,54,98,99] To some extent, this is also the case for Anderson-type POMs,[52] where the LUMO is localized on the central heterometal. In these cases, the POM–PS hybrids showed absorption/emission dominated by the PS in the visible range, indicating negligible electronic interaction with the POM unit in the ground state. The modification of the organic moieties does not influence the redox properties of the POM (unless in case of charged organic PS, in which the redox potentials are affected by electrostatic interactions between the charged-subunits).[65] Similarly, for polyoxovanadotungstate Dawson $[P_2W_{15}V_3O_{62}]^{9-}$ with triol-based ligands, the HOMO was found to be localized on the organic moieties and the LUMO was localized on the V_3 cap.[30,76] Note that in the case of hexavanadates, some electronic interaction between the POM core and the triol-based ligand has been observed.[100,101]

Other examples in which organic functionalization modified the redox properties of the POM, to some extent, are also reported in the literature. The first case is the imido functionalized hexamolybates, as developed by the groups of Peng,[59,60] Wei[102] and Fielden.[103] In this case a DFT study showed that the Mo≡N functionalization participate both to the HOMO (mostly localized on the PS) and the LUMO.[104] Another example is the insertion of an amide bond on a polyoxovanadotungstate Dawson $[P_2W_{15}V_3O_{62}]^{9-}$.[105] Here, it was found that the modification of the organic moieties could tune the first reduction wave of the POM by up to 50 mV. Finally, the redox properties of organophosphonate[92,106] and organoarsonate[21] derivatives of POMs were found to differ even more according to the nature of the organic moieties grafted to the POM. The involvement of the P and As atoms and the mixing between the organic and inorganic components in the frontier molecular orbitals was evidenced by time dependant-DFT calculations[21,92] (Fig. 3). Consequently, in these hybrid POMs, the electronic interactions between the organic part and the POM unit are responsible of the visible absorption.

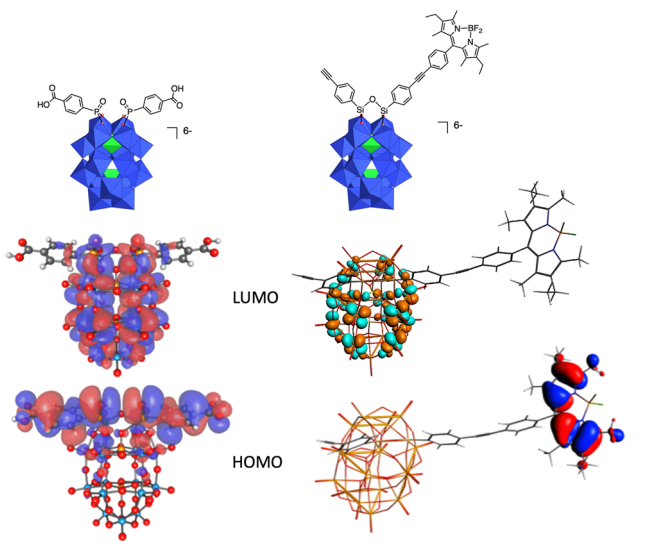

Fig. 3 (Left) Frontier molecular orbitals of a redox coupled organophosphonate hybrid. Reproduced from ref. 92 with permission from American Chemical Society, copyright 2017 . (Right) Frontier molecular orbitals of a redox decoupled organosilane Dawson-bodipy derivative. Reproduced from ref. 54 with permission from John Wiley and Sons, copyright 2021.

3 Kinetics of monoelectronic photoinduced electron transfers

As for any donor–acceptor system, the evaluation of the kinetics of photoinduced electron transfers in POM–PS assemblies can be estimated by the luminescence quenching of the PS (in terms of the quantum yield or luminescence lifetime) or more directly by transient absorption spectroscopy (TAS). TAS provides both the spectroscopic signatures and kinetics of relaxation of the different photoexcited states (see Table 1). While TAS is very well-established, the unambiguous evaluation of the formation of charge-separated state in POM–PS assemblies may be challenging, as reduced forms of POMs have often broad absorption in the NIR region with rather low extinction coefficient (1000–8000 M^{-1} cm^{-1}). Consequently, the monitoring of the kinetics of photoinduced electron transfer is often followed using the signature of the oxidized chromophore, which for organic dyes is typically more intense and well-resolved.

In Sections 3 and 4 we will mainly focus on POM–Ir(III)[51] and POM–bodipy[54] hybrids as case studies. Indeed, for these hybrid POMs, the kinetics of both monoelectronic charge separation/recombination but also their abilities to perform charge photoaccumulation[26,110] are reported and quantified. These systems will provide insightful information regarding the advantages and limitations of the development of POM–PS for artificial photosynthesis.

3.1. Multimolecular POM–PS and TMS-POMs

In addition to the challenges of unpicking competing dynamic and static electron transfer in electrostatic and coordination bond adducts, the presence of free PS in diluted solutions may lead to persistent, overlapping signals that evolve in the nanosecond timescale that again complicates the analysis.[33] In these

Table 1 Selected parameters relevant for the CS and CR steps for the POM–PS assemblies reported in the literature, τ being the time constant $\tau = 1/k$

	Reference/ label in Fig. 6	POM	PS	solvent	E° (PS^+/PS)/ V *vs.* SCE	E° (POM/POM + 1 e)/V *vs.* SCE	$-\Delta G^0_{CS}$/eV	τ_{CS}/ns	$-\Delta G^0_{CR}$/eV	τ_{CR}/ns
Non	32	$[SiW_{11}O_{39}Co(OH_2)]^{6-}$	$[(Rubpy)_3]^{2+}$	H_2O/LiCl		−0.88	0.20	12 ns	Not reported	
covalent	32	$[PW_{11}O_{39}Mn(OH_2)]^{6-}$	$[(Rubpy)_3]^{2+}$	H_2O/LiCl		−1.02	0.34	<2 ns	Not reported	
	32	$[SiW_{11}O_{39}Co(OH_2)]^{6-}$	$[(Rubpy)_2(4,4'\text{-}Cl_2bpy)]^{2+}$	H_2O/LiCl		−0.88	0.07	250	Not reported	
	32	$[PW_{11}O_{39}Mn(OH_2)]^{6-}$	$[(Rubpy)_3]^{2+}$	H_2O/LiCl		−1.02	0.21	<5 ns	Not reported	
	38	$[PW_{12}O_{40}]^{3-}$	Tin(IV)-porphyrin	PhCN	0.69	−0.48	0.68	0.2	Very fast	
	38	$[PW_{12}O_{40}]^{3-}$	Tin(IV)-porphyrin	PhCN	0.86	−0.50	0.48	CS much slower than the ISC (~0.1 ns)		
	40	$[PW_{12}O_{40}]^{3-}$ 5 equiv.	$[Mo_6I_8Cl_6]^{2-}$	MeCN	~1.00[a]	~−0.17[a]	0.6	23×10^3	1.17	350×10^3
	40	$[PW_{18}O_{62}]^{6-}$ 5 equiv.	$[Mo_6I_8Cl_6]^{2-}$	MeCN	~1.00[a]	~−0.57[a]	0.2	42 × 103	1.57	620×10^3
	40	$[BW_{12}O_{40}]^{5-}$ 5 equiv.	$[Mo_6I_8Cl_6]^{2-}$	MeCN	~1.00[a]	~ −1.07[a]	−0.3	No CS formed		
	107	$[Mo_6O_{19}]^{2-}$	Ferrocenyl cation	Sol. state (alum.)	Charge transfer band at 550 nm			$\ll 25 \times 10^{-3}$		$\sim 25 \times 10^{-3}$
	108	$[Mo_6O_{19}]^{2-}$	Pyrene cation	Cryst. mat.	Charge transfer band at 500–600 nm			$\ll 25 \times 10^{-3}$		56×10^{-3}
	108	$[Mo_6O_{19}]^{2-}$	Pyrene cation	Cryst. mat.	Charge transfer band at 500–600 nm			$\ll 25 \times 10^{-3}$		0.20
Coord. Bond	48	$[CoSiW_{11}O_{39}]^{6-}$	Porphyrin	$C_2H_4Cl_2$	Not given			60×10^{-3}	Not given	
TMS-POM	86	$[P_4W_{35}O_{124}\{Re(CO)_3\}_2]^{16-}$		CH_2Cl_2	Charge transfer band up to 600 nm			35×10^{-6}		1.4×10^{-3}
	87	$[SiW_{11}O_{39}Co^{II}(H_2O)]^{6-}$		H_2O						1.3×10^{-3}
	87	$[Co^{II}W_{12}O_{40}]^{6-}$		H_2O						0.42
	87	$[Co^{II}W_{12}O_{40}]^{6-}$		MeCN						1.7
Covalent	63	$[P_2W_{17}O_{61}\{O(SiPS)_2\}]^{6-}$	Perylene monoimide	DMF	1.00[a]	−0.84[a]	0.34	40% fluor. quench. diff. CS rates (ps–ns)	1.84	Faster than CS
	63	$[P_2W_{17}O_{61}\{POPS\}_2]^{6-}$	Perylene monoimide	DMF	1.00[a]	Not given, estim. to −0.46 V	0.87	97% fluor. quench. $\sim 70 \times 10^{-3}$	~1.33	0.16
	25	$[P_2W_{17}O_{61}\{O(SiPS)_2\}]^{6-}$	Zn(II)-porphyrin	DMF	0.70	−0.68	S_1 0.68 T_1 0.18	$\tau_1 \sim 0.50$ $\tau_2 \sim 3.8$	1.38	Faster than CS
	25	$[P_2W_{17}O_{61}\{POPS\}_2]^{6-}$	Zn(II)-porphyrin	DMF	0.72	−0.18	S_1 1.16 T_1 0.66	$\tau_1 = 0.1$ $\tau_2 = 22$	0.9	Faster than CS
	25/P	$[P_2W_{17}O_{61}\{POPS\}_2]^{6-}$	Zn(II)-porphyrin	DMF	0.71	−0.30	S_1 1.05 T_1 0.55	22	1.10	Faster than CS
	51/M	$[PW_{11}O_{39}\{O(SiPS)_2\}]^{3-}$	Cyclometalated Ir(III)	DMF	1.05	−0.38	1.00	3.9×10^{-3}	1.43	1.5
	51/F	$[P_2W_{17}O_{61}\{O(SiPS)_2\}]^{6-}$	Cyclometalated Ir(III)	DMF	1.03	−0.73	0.67	0.5	1.76	27
Covalent	51/C	$[PW_{11}O_{39}\{(SnPS)\}]^{4-}$	Cyclometalated Ir(III)	DMF	1.05	−1.09	0.29	46	2.14	180
	51/B	$[P2W_{17}O_{61}\{(SnPS\}]^{7-}$	Cyclometalated Ir(III)	DMF	1.01	−1.28	0.14	82	2.29	480
	31/O	$[PMo_{11}O_{39}\{SnPS\}]^{4-}$	Cyclometalated Ir(III)	DMF	1.29 (irr)	−0.51	0.30	67		
	53/D	$[PMo_{11}O_{39}\{(SnPS)\}]^{4-}$	Bodipy	CH_2Cl_2	1.02	−0.57	0.56	0.18	1.55	0.52 (evol. into PS triplet state)
	53	$[PW_{11}O_{39}\{(SnPS)\}]^{4-}$	Bodipy	CH_2Cl_2	0.98	−1.11	0.03	No CS formed		
	68/J	$[PMo_{11}O_{39}\{(SnPS)\}]^{4-}$	Bodipy	MeCN	~1.02	−0.99	0.86	2.2	1.48	16
	68	$[PW_{11}O_{39}\{(SnPS)\}]^{4-}$	Bodipy	MeCN	~1.02	−0.48	0.35	No CS formed		
	54/N	$[PW_{11}O_{39}\{O(SiPS)_2\}]^{3-}$	Bodipy	MeCN	1.01	−0.33	1.02	38×10^{-3}	1.32	1.3
	53 and 54/L	$[PW_{11}O_{39}\{O(SiPS)_2\}]^{3-}$	Bodipy	CH_2Cl_2	1.02	−0.45	0.94	54×10^{-3}	1.39	4.8
	54/K	$[PW_{11}O_{39}\{O(SiPS)_2\}]^{3-}$	Bodipy	DMF	1.03	−0.36	0.95	2.0	1.39	5.7
	54/I	$[P_2W_{17}O_{61}\{O(SiPS)_2\}]^{6-}$	Bodipy	MeCN	0.99	−0.57	0.80	0.38	1.54	3.1
	54/G	$[P_2W_{17}O_{61}\{O(SiPS)_2\}]^{6-}$	Bodipy	CH_2Cl_2	1.00	−0.71	0.70	0.34	1.63	13
	54/E	$[P_2W_{17}O_{61}\{O(SiPS)_2\}]^{6-}$	Bodipy	DMF	1.03	−0.69	0.62	2.4	1.70	10

Table 1 (*Contd.*)

Reference/ label in Fig. 6	POM	PS	solvent	E° (PS^{+}/PS)/ V *vs.* SCE	E° (POM/POM + 1 e)/V *vs.* SCE	$-\Delta G^{0}_{CS}$/eV	τ_{CS}/ns	$-\Delta G^{0}_{CR}$/eV	τ_{CR}/ns
50 and 82/A	$[PW_{11}O_{39}\{(GePS)\}]^{4-}$	Ru(II) bis terpyridine	DMSO	1.22	−0.99	0.11	32	2.21	470
28/H	$[P_2W_{17}O_{61}\{POPS\}_2]^{2-}$	Ru(II) tris bipyridine	DMF	1.10[a]	−0.21[a]	~0.7	12×10^{-3}	1.31	0.09
49/Q	$[P_2V_3W_{15}O_{59}\{(OCH_2)_3PS\}]^{-}$	Zn(II)-porphyrin	DMF	0.81	−0.03[a]	S_2 1.97 S_1 1.13	2.3×10^{-3} 62×10^{-3}	0.84	>1 ns
49	$[MnMo_6O_{18}\{(OCH_2)_3PS\}]^{-}$	Zn(II)-porphyrin	DMF	0.86	−1.17[a]	S_2 0.93 S_1 0.09	No CS formed		
52 and 79	$[MnMo_6O_{18}\{(OCH_2)_3PS\}]^{-}$	Cyclometalated Ir(III)	DMF	1.37[a]	−0.83[a]	Hot state ≫0.13 ^{3}MLCT 0.13	0.5×10^{-3} —	2.20	0.29
52 and 79	$[FeMo_6O_{18}\{(OCH_2)_3PS\}]^{-}$	Cyclometalated Ir(III)	DMF	1.37[a]	−0.95[a]	Hot state ≫0.01 ^{3}MLCT 0.01	0.5×10^{-3} —	2.32	0.43
52 and 79	$[CoMo_6O_{18}\{(OCH_2)_3PS\}]^{-}$	Cyclometalated Ir(III)	DMF	1.37[a]	−0.84[a]	Hot state ≫0.12 ^{3}MLCT 0.12	0.5×10^{-3} —	2.21	0.54
80 and 109	$[MnMo_6O_{18}\{(OCH_2)_3PS\}]^{-}$	Cyclometalated Ir(III)	DMF	1.33[a]	−0.76[a]	0.24	0.18	2.09	<0.18

[a] Redox potential extrapolated to SCE reference.

cases, the evaluation of the luminescence quenching using time-resolved photoluminescence spectroscopy allows the estimation of the kinetics of both dynamic and static quenching although the decrease in quantum yield represents the global quenching process. In some studies, authors have observed that, depending on the experimental conditions, luminescence intensity could decay by a mono or a bi-exponential function with lifetimes for electron transfer ranging from tens of picoseconds[48] to few nanoseconds.[32] The case of porphyrin PS is even more complex as both singlet and triplet state can be potentially quenched by the POM. In this case, it was found that, depending on the driving force in the photoinduced electron transfer, the quenching could be rather efficient from the singlet state with photoinduced electron transfers of *ca.* 0.2–1 ns, compared to the triplet state (displaying a lower energy), with lifetimes estimated to be *ca.* 100 ns.[38]

In few cases, where the POM-based system was an electrostatic adduct[33,107,108] or a TMS-POM,[86] the authors observed new optical features, putatively assigned to a charge transfer (CT) transition, as the absorption spectrum of the whole system differed from the sum of the individual subunits. In one case, the authors indicated that such transition led to a luminescent CT state.[33] The unambiguous characterization of charge-separated states by TAS of multimolecular POM–PS assemblies was only seldomly reported.[40,107,108] In the case of a ferrocenyl/$[Mo_6O_{19}]^{2-}$ adduct, TAS of the material in the solid-state indicated that the resulting charge-separated (CS) state displayed very short lifetime (in the ps timescale) because of the close proximity between the POM and the electron donating unit. A similar feature was observed for a series of crystalline materials associating cationic polyaromatic compounds (anthracene, pyrene) to Lindqvist-type ($[W_6O_{19}]^{2-}$, $[Mo_6O_{19}]^{2-}$) and Keggin-type POMs ($[SiW_{12}O_{40}]^{4-}$, $[SiMo_{12}O_{40}]^{4-}$).[108] In this instructive study, the authors correlated the distance between the POM and the polyaromatic moieties to the coloration of the compound in the solid state and to the kinetic of charge recombination. It was inferred that the shorter the POM–polyaromatic compound distance, the darker the colour of the crystal and the faster the decay of the CT state. Using a similar POM ($[Mo_6O_{19}]^{2-}$)/cationic pyrene combination, two polymorphic crystalline materials were isolated, each one featuring different POM–pyrene distances, coloration (orange/yellow, red) and kinetics of CR (50/200 ps).

In the case of the association of Keggin- and Wells–Dawson-type POMs to anionic electron rich $[Mo_6I_8Cl_6]^{2-}$ cluster, charge-separated states with very long lifetime were observed (hundreds of μs, Table 1).[40] The long-lived character of the CS state is probably due to the low affinity between both polyanionic species in solution. The authors demonstrated that for this specific case of POM–PS, the cluster quenching could be correlated with the charge density of the POM and not its redox property.

In TMS-POMs, the systems often displayed very short lifetime again probably owing to the close proximity between the POM and the transition metal.[86,107] For instance, excitation at 400 nm of $[P_4W_{35}O_{124}\{Re(CO)_3\}_2]^{16-}$ or $[P_2W_{17}O_{61}\{Re(CO)_3\}_3\{ORb(H_2O)\}(\mu_3\text{-}OH)]^{9-}$ showed the instant formation of CS states

with very short lifetime (below 10 ps) as evidenced by TAS.[86,90] Longer-lived CT excited states have been described for Co-containing Keggin POMs, with a clear effect of the substitution site, either at the tetrahedral site or at a pseudo-octahedral addendum position.[87] The dynamics of the excited states of $[Co^{II}W_{12}O_{40}]^{6-}$ and $[SiW_{11}O_{39}Co^{II}(H_2O)]^{6-}$ have been monitored after excitation at 400 nm. Both species exhibited a bi-exponential decay, with a first excited state decaying in a few hundreds of fs and a second longer-lived intermediate assigned to a CT state. The longer lifetime observed in $[Co^{II}W_{12}O_{40}]^{6-}$ is consistent with the ability of the central Co to undergo structural distortion and to display poor orbital overlap between the tetrahedral site and the reduced tungstate framework. A putative transient valence-trap with the excited electron localized on a single tungsten among the twelve was also proposed to explain the slower CR (τ = 420 ps in H_2O, τ = 1700 ps in MeCN) of excited $[Co^{II}W_{12}O_{40}]^{6-}$ compared to that of excited $[SiW_{11}O_{39}Co^{II}(H_2O)]^{6-}$ (τ = 1.3 ps in H_2O). Later investigation of the heterobimetallic TMS-POMs $[Co^{II}W_{11}O_{39}\{(M^xOH_y)\}]^{(12-x-y)-}$ (MOH_y = $V^{IV}O$, $Cr^{III}(OH_2)$, $Mn^{II}(OH_2)$, $Fe^{III}(OH_2)$, $Co^{II}(OH_2)$, $Ni^{II}(OH_2)$, $Cu^{II}(OH_2)$, $Zn^{II}(OH_2)$), did not show any improvement of the lifetime (sub-300 ps in aqueous media), probably due to the increase of the anion charge and ion-pairing.[111] Excited state with even longer lifetime (τ = 20 ns) could be observed in the case of $[X\{Bi(dmso)_3\}_2V_{12}O_{33}]^-$,[89] in which the Bi(III) centre is not involved in the excited state solely localized on the dodecavanatade framework.

3.2. Covalent POM–PS

The evaluation of the kinetics of electron transfer in covalent POM–PS assemblies provide more information on the behaviour of POMs as electron acceptors. Typically, POM–PS hybrids using Keggin- and Wells–Dawson-type POMs with organosilane, organotin and organophosphonate functional anchoring groups gave insightful information regarding the kinetics of photoinduced electron transfer. When the POM and PS were linked through flexible organic bridges to perylene monoamide or Zn(II) porphyrin,[25,63] the emission decay curves were found to be non-exponential. This was attributed to the presence of multiple conformers. Furthermore, no spectroscopic signature for a CS state could be observed with such systems. Indeed, the CR in such flexible POM–PS assemblies could probably be very fast due to a folding of the oxidized PS to the POM, as already evidenced in a mesogenic donor–acceptor hybrid system.[71] When the Keggin or Wells–Dawson-type POM and the PS were connected through a rigid organic spacer, the CS state could sometimes be unambiguously determined by comparing the experimental TAS absorption spectra to the simulated spectra (*i.e.* the sum of the spectra of the mono-reduced POM and the oxidized PS) of the CS state (Fig. 4).

Among the developed POM–PS systems, the TAS study of those based on porphyrin were difficult to investigate owing to the complex relaxation dynamics (S_2–S_1, ISC) involved in these systems. Consequently, the persistence at long timescale of the signal of the porphyrin triplet state often hindered the observation of the CS state. Nevertheless, several studies with organic dyes or organometallic complexes allowed the kinetics of both CS and CR to be estimated in these POM–PS assemblies.

In the non-adiabatic limit (*i.e.* when the hybridization between D and A is limited), the rate constant for an electron transfer process between a donor (D) and acceptor (A) is described by the Marcus theory,[112,113] and the driving force of the CS (ΔG^0_{CS}) and CR (ΔG^0_{CR}) are estimated using the Rehm–Weller equations.[114,115]

$$k = \nu \exp\left(\frac{-\left(\lambda + \Delta G^0_{ET}\right)^2}{4\lambda RT}\right)$$

$$\Delta G^0_{CS} = E_{ox}(D) - E_{red}(A) - E_{00} - w_{el}$$

$$\Delta G^0_{CR} = E_{red}(A) - E_{ox}(D) + w_{el}$$

ν the electronic frequency depends, (among other parameters) on the overlap between the electronic wavefunction of the donor and acceptor units, λ is the reorganization energy and ΔG^0_{ET} is the free energy of the electron transfer. E_{00} is the energy of PS*. The work term for electrostatic interactions w_{el} is often neglected in polar organic solvent. For polyanionic species, the exact evaluation of the reorganization energy is particularly challenging as it requires the exact distances between all charged species to be known, including the counter ions associated with the POMs. As a first approximation, it can be considered that the associated counter ions screen the charges of the POM and that the POM/counter ions behave as a global neutral species. Using such an approximation, when the distance between the POM and the PS is *ca.* 2 nm, the work term is calculated to be 0.08 eV in CH_2Cl_2 and 0.02 eV in MeCN and DMF, which probably underestimates its actual value.[54] The redox and photophysical properties of all reported systems are reported in Table 1.

Our group reported the photophysical properties of a series of four POM–Ir(III) covalent assemblies (Fig. 4).[51] The same cyclometalated Ir(III) complex was grafted on four hybrid platforms displaying distinct electron accepting properties. In these molecular systems in which the POM and the PS were electronically decoupled, we found that the CS rate increased with $|\Delta G^0_{CS}|$ (ranging from 0.14 eV to 1.00 eV) while the CR rate decreased with $|\Delta G^0_{CR}|$. This suggested, assuming a similar reorganization, that the CS process occurred in the Marcus normal region ($|\Delta G^0_{CS}| < \lambda$) while the more exergonic CR were located in the Marcus inverted region ($|\Delta G^0_{CR}| > \lambda$). In this specific case, it was also found that because of the heteroleptic character of the Ir(III) complex, the photoinduced electron transfer was favoured for the CS and delayed for the CR (Fig. 5), as the overlap between the electronic wavefunctions of the donor and acceptor groups differed in the Ir(III) excited state (donor: reduced picolinate ligand; acceptor: POM) and the CS state (donor: reduced POM; acceptor, oxidized Ir-phenylpyridine). The directionality in the photoinduced electron transfer is indeed a key parameter to obtain efficient charge photoaccumulation (see Section 4).

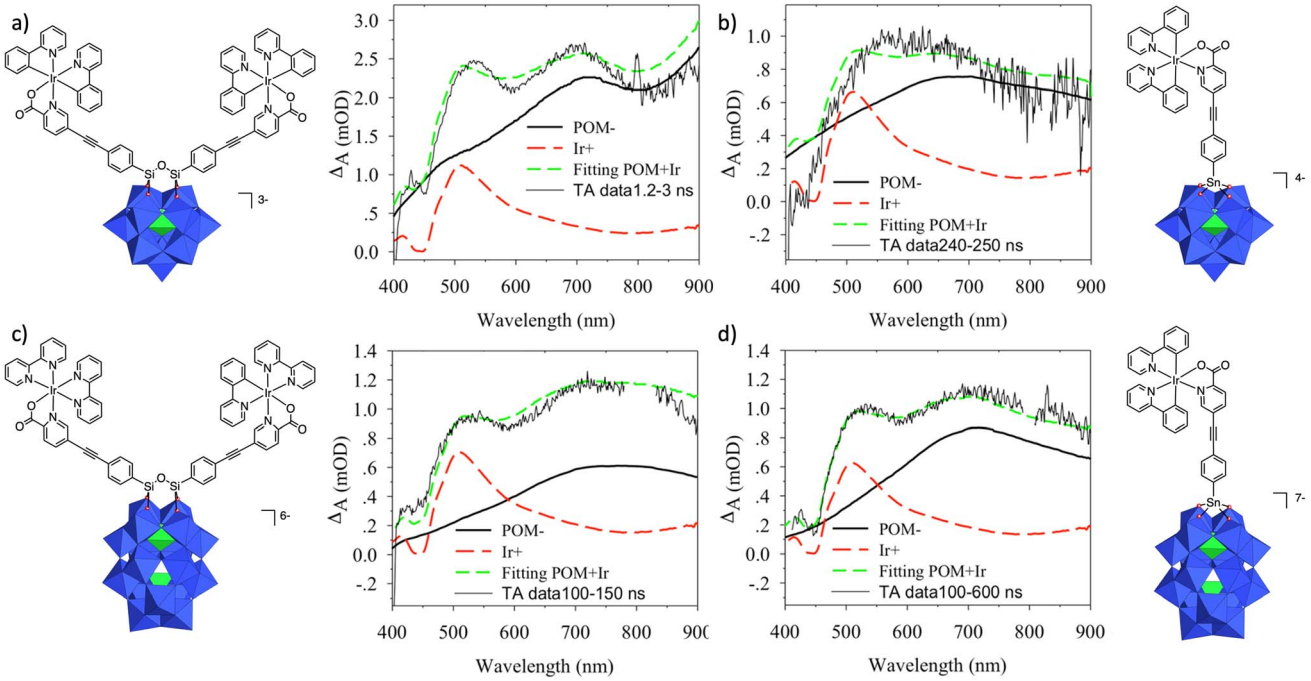

Fig. 4 Comparison of transient absorption spectra (thin black solid line) at indicated delay time and simulated spectra (green dashed line) of charge-separated states in for POM–Ir(III) hybrids: (a) Keggin-organosilane, (b) Keggin-organotin, (c) Dawson-organosilane, (d) Dawson-organotin. The simulated spectra are a sum of the spectrum of the mono-reduced POM (thick black solid line) and the oxidized iridium references (red dashed line). Reproduced from ref. 51 with permission from the Royal Society of Chemistry, copyright 2013.

More recently a series of POM–bodipy hybrids were developed to avoid the use of noble metals. A similar trend (*i.e.* the CS and CR rates respectively increased and decreased with the driving force) was observed on these hybrids.[53,54,68] In a work that combined experimental and theoretical approaches,[54] the reorganization energy was estimated to be *ca.* 0.94–1.24 eV according to the nature of the POM or the solvent. Actually, the difference in reorganization energy was found to be *ca.* 0.05 eV smaller for the Wells–Dawson-type hybrids compared to the Keggin ones. This system was further investigated to evaluate the effect of the POM counter ion and solvent on the kinetics of photoinduced electron transfer (*vide infra*).

Other reports using TAS include Keggin- and Wells–Dawson-type POM connected to Ru(II) polypyridyl complexes,[28,50] and Dawson-type POMs coupled to porphyrins.[25,49] Very interestingly, when plotting the kinetics of CS and CR (when the charge-separated state was observed) in the logarithmic scale ($k_{ET} = 1/\tau$ with τ values listed in Table 1) according to the driving force of the electron transfer for all these hybrid systems, a correlation can be observed (Fig. 6). The slower CS processes are associated with small driving force (below 0.5 eV), while fast CS processes (below 100 ps) are only observed when the driving force is *ca.* 1 eV. Conversely systems with slow CR (above 10 ns) were found to display high driving force. In other words, systems that displayed high-energy charge-separated state (*i.e.*, when POMs have low electron accepting properties) are slow for both CS and CR, while those based on POMs with good electron accepting properties, are fast for both electron transfer processes. The deviation from the observed trend is probably due to the difference in the chemical bridge between the POM and the PS (distance, conjugation, decoupling of the electronic state, directionality, *etc.*) and also the difference in solvent (*vide infra*) that has a significant effect on the photophysical properties in these systems.

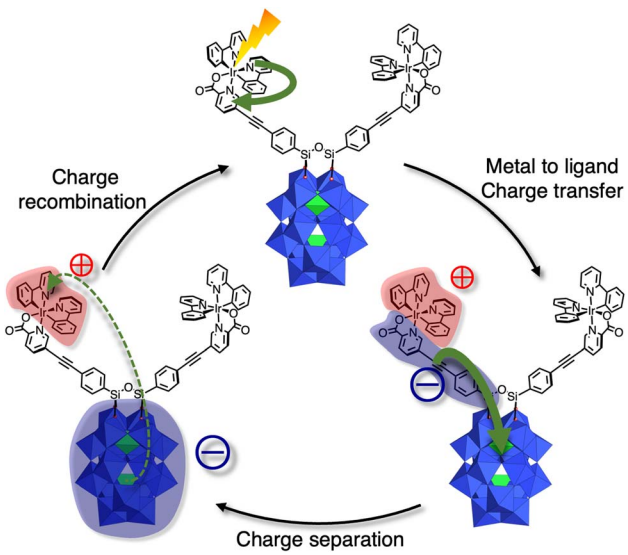

Fig. 5 Directionality in the photoinduced electron transfers of the POM–Ir(III) assembly $[P_2W_{17}O_{61}\{O(SiC_{36}H_{23}O_2N_3Ir)_2\}]^{6-}$, conferred by the heteroleptic character of the Ir(III) complex. The red and blue cloud respectively represent the localization of the positive and negative charges in the different excited states.[51]

The photophysical properties of Anderson-type POM-based hybrid are more complex. This may arise from the fact that while in most reduced POMs the added electron is delocalized onto the whole POM framework, in Anderson–Evans, the first reduction corresponds to a process localized on the central metal (*e.g.* Mn(III), Co(III), Fe(III)). Consequently, the intrinsic electron delocalization of reduced forms of POMs is not present in mono-reduced Anderson systems, resulting in very unusual behaviour of the photosensitized hybrids. In some cases, no quenching of the excited PS (porphyrin,[49] bodipy[116,117]) was observed owing to the rather negative potential of the reduced POM. By contrast with Ir(III) cyclometalated chromophores some partial, if not total, quenching of the luminescence was observed depending on the organic spacer between the POM and the PS. With an imine spacer, the reminiscence of the ^{3}MLCT state with the same lifetime as the parent chromophore, suggested that this relaxed excited state is not responsible of the luminescence quenching. Indeed, with this relaxed excited state the driving force for the CS is very low (less than 0.15 eV). The authors attributed the partial formation of a charge separated state with a very fast process (*ca.* 0.5 ps) from a hot ^{3}MLCT$_{ppy}$ state[79] even though the energy of hot excited state was estimated by other authors to be rather close to that of the relaxed ^{3}MLCT$_{ppy}$ state.[118] The resulting POM–Ir charge-separated state displayed very short-lived character (<1 ns) while its energy is very high. More recently, the authors also evaluated the effect of the modification of the organic linker.[80] Using a shorter organic tether between the Ir(III) photosensitizer and the POM, they observed an almost total quenching of the Ir(III) luminescence that can be attributed to a more efficient electron transfer from the photo-excited PS to the POM. From femtosecond TAS, the authors concluded that the CS was operative from the relaxed ^{3}MLCT$_{ppy}$ state with a kinetic of 180 ps. Yet with this system, the charge-separated state could not be observed, indicating that it would recombine at a faster pace.

Finally, the photophysical properties of an elegant POM-based molecular capsule consisting of diarylethene sandwiched by two trivacant lacunary phosphomolybdate [A-α-PMo$_9$O$_{34}$]$^{9-}$ was recently reported.[55] This system features interesting photophysical behaviour as the diarylethene can either act as an electron donor or as a photochromic unit. Furthermore, the formation of triplet species was also proposed. In this article, the authors propose the formation of a charge separated state with an intriguing lifetime exceeding 200 μs, which exceed by far the values of all previously mentioned systems.

From the comparison of all the covalent POM–PS systems, it is found that those based on larger POMs (Keggin and Wells–Dawson structures) display the longest charge-separated state. This outlines the importance of the electron delocalization of the reduced POMs in the kinetics of photoinduced electron transfers with POM–PS hybrids. The comparison of two different PS (cyclometalated Ir(III) complex and bodipy) can be made on similar hybrid platforms and in the same solvent.[51,54] It can be clearly found that the τ_{CR}/τ_{CS} ratio is considerably higher for the organometallic PS (τ_{CR}/τ_{CS} in the range of 50–380) as it displays directional electron transfer (Fig. 5), a feature that is absent in the bodipy dye (τ_{CR}/τ_{CS} in the of range 3–4). For these POM–PS systems, only fast photoinduced electron transfer (below 100 ps) could be observed when the driving force for the charge separation was important (*ca.* 1 eV), which implies that (i) some energy loss is necessary to ensure efficient electron transfer, (ii) only high-energy excited state PS and hybrid POMs with good electron accepting properties can lead to rapid photoinduced charge separation.

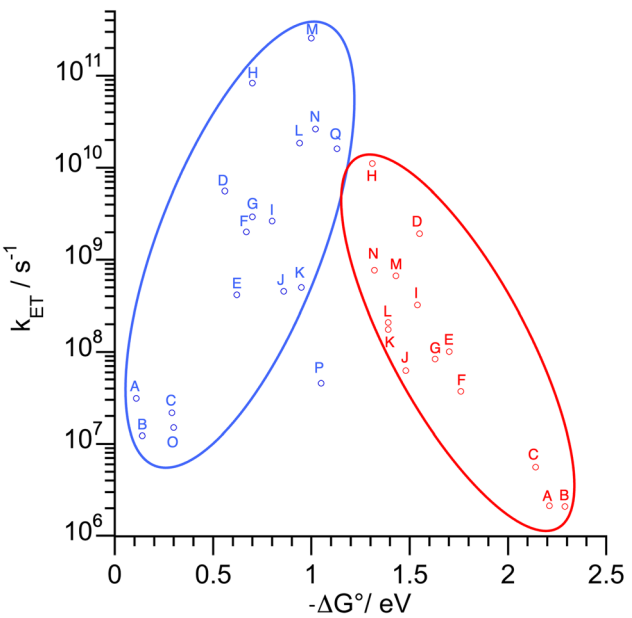

Fig. 6 Correlation between kinetics of CS (blue circles) and CR (red circles) and the thermodynamic driving force ($-\Delta G^0$) in covalent POM–PS assemblies based on Keggin and Wells–Dawson structures according to Table 1. The alphabetic labels correspond to the same compound (see Table 1). Note that for points labelled O, P, Q the kinetics of CR is not reported in the literature.

3.3. Environmental effects (solvent, counter ion) on the electron transfer kinetics

The environment influences the CS kinetics between POMs and PS, as revealed by a combination of experimental techniques and theoretical investigations.[53,54,68,119,120] Both the solvent and associated counter ions significantly impact the energy of the charge-transfer state by modifying the solvation shell around the POMs, which constitutes another source of richness of POM chemistry. This can be rationalized using abovementioned Marcus theory, demonstrating that solvent and counter ion variations affect both the driving force for photoinduced electron transfer and the reorganization energy. It is understood that solvent and electrolyte choice significantly influence redox potentials of POMs, due to specific solvation and entropic effects, differences in viscosity and reorganization energy, ion pairing and coordination.[13,121–124]

To illustrate this, organosilane hybrid derivatives incorporating Wells–Dawson and Keggin POMs were compared in CH_2Cl_2, DMF and MeCN (with tetrabutylammonium (TBA) hexafluorophosphate electrolyte), and the first two reductions found to be shifted by *ca.* 115–160 mV for these hybrids.[54]

Changing the electrolyte also altered the redox behaviour. In DMF, switching from $TBAPF_6$ to tetraethylammonium (TEA) perchlorate and tetramethylammonium (TMA) tetrafluoroborate shifts the Dawson-based hybrid's first reduction by 230 mV. Molecular dynamics simulations revealed closer cation–POM interactions with smaller cations (TMA, TEA) than with bulky TBA. Solvent effects varied but the observed trends were consistent with coordination numbers and interaction energies, with TBA having weaker binding to the POM (especially in MeCN) but stronger solvent affinity (especially in DMF). DFT calculations showed that the LUMO energy of the hybrids depended on solvent polarity and number of POM-contacting counterions, with stronger ion pairing (for the smaller cations) leading to a lower LUMO. This sensitivity adds complexity to photophysical behaviour, influencing both the reorganization energy (λ ~0.94–0.99 eV in CH_2Cl_2 to 1.19–1.24 eV in MeCN due to differences in polarity for the Keggin- and Wells–Dawson-bodipy) and thermodynamics of photoinduced electron transfer. In CH_2Cl_2 and MeCN, bodipy fluorescence was similarly quenched (~85%) due to efficient CS. The similar CS rates in CH_2Cl_2 and MeCN suggest that CH_2Cl_2 compensates for its lower driving force with a lower λ. By contrast it was found that the charge-separated state lasts 3–4 times longer in CH_2Cl_2 than in MeCN. This is because, in CH_2Cl_2, CR has lower reorganization energy and a higher driving force. Since recombination occurs in the Marcus inverted region, both factors raise the activation energy, extending the excited state lifetime. In DMF, both excited-state decay and CS were surprisingly slow though DMF's redox potentials and λ values fall between those of CH_2Cl_2 and MeCN. In this case, it was proposed that the high viscosity of DMF and the strong TBA solvation likely hinder rapid counterion rearrangement, slowing electron transfer. Simulations confirm that in DMF, TBA cations are largely in the bulk, unlike in CH_2Cl_2, where they remain near the POM. This suggests that slow ion exchange in DMF acts as a gating mechanism for ET. The counterions also influenced the kinetics. In DMF, the TMA salt of the Dawson-bodipy showed faster decay than TEA or TBA analogues. In MeCN, TMA accelerated CS the most. In CH_2Cl_2, a mixed TMA/TBA salt displayed extremely fast charge injection (~4 ps), but the result may be confounded by aggregation. Although solubility was limited, this hybrid displayed both ultrafast CS and long-lived charge-separated states, making it the most efficient system studied.

Photoinduced electron transfer in Keggin hybrids can also be modulated by protonation, shown with POM–bodipy and POM–Ir(III) organotin hybrids.[31,68] The findings are consistent with proton-coupled electron transfer (PCET), where the interplay of protonation and electron transfer governs the CS and CR processes. In the polyoxomolybdate-based POM–bodipy hybrid, photoinduced CS occurred spontaneously in solution, while in the polyoxotungstate analogue, electron transfer was inefficient due to a poorer electron accepting property of the latter.[68] A similar feature was later observed with POM–Ir(III) hybrids.[31] Protonation (in this case *via* addition of trifluoroacetic acid (TFA)), shifts the redox potential of the POM to more positive values, enhancing the thermodynamic driving force for light-induced electron transfer (Fig. 7). In the polyoxotungstate–bodipy hybrid, TFA enables partial CS, but the driving force remained insufficient for high efficiency, and CR in tens of ns led to the formation of bodipy triplet states due to tungsten's heavy atom effect. In contrast, for the polyoxomolybdate analogue, TFA drastically accelerated CS (from 2.2 ns in the absence of acid down to 91 ps), and CR slowed (up to 1.3 μs), plateauing at 500 equivalents of TFA. A polyoxomolybdate–Ir(III) hybrid showed a similar trend albeit the increase in the electron transfer upon the addition of an acid source was less pronounced (CS accelerated from 60 ns in the absence of proton down to 26 ns in the presence of 250 equiv. TFA).[31] In these hybrids, charge-separation enhancement with acid likely occurs *via* sequential proton transfer and electron transfer, while charge-recombination appears to involve a concerted or sequential mechanism influenced by POM basicity. Weak interactions between H^+ and oxidized POMs complicate full protonation at low acid concentrations. A detailed theoretical investigation of the intricate mechanism of the protonation step in the excited state would be of high interest to account for these experimental findings.

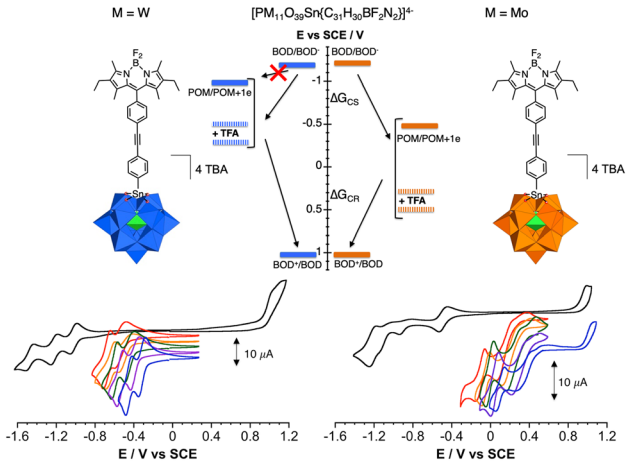

Fig. 7 (Top) Energy level diagram of the polyoxotungstate- (blue) and poloxomolybdate- (orange) bodipy hybrids showing the effect of the presence of TFA in MeCN. (Down) Cyclic voltammograms of the POM–bodipy hybrids (black curves, top panel) 1 mM in MeCN containing 0.1 M $TBAPF_6$ solutions and after the addition of 30 (red), 60 (orange), 100 (green), 200 (purple) and 500 (blue) equiv. of trifluoroacetic acid (TFA); working electrode: glassy carbon; reference electrode: SCE. Reproduced and adapted from ref. 68 with permission from the Chinese Chemical Society (CCS) Peking University (PKU), and the Royal Society of Chemistry, copyright 2021.

4 Charge photoaccumulation/ electron release

One exciting potential of POM–PS hybrids is their capacity for charge photoaccumulation – an essential feature for solar fuel production and water splitting, which rely on the catalysis of multielectron, multiproton reactions. Because POMs can undergo multiple reversible reductions without significant structural rearrangement, they can stably maintain higher reduced states enabling storage of several electrons. Developing

POM–PS systems for charge accumulation, however, remains scarcely explored, due to several energetic and kinetics constraints that necessitate complex design.

Two main strategies have been followed when developing molecular systems able for charge photoaccumulation.[125–127] The most prevalent one relies on the use of sacrificial electron donors (SEDs), in large excess, to efficiently reduce the charge-separated state, thereby minimizing charge recombination and promoting the formation of the targeted photoproducts. This method, as demonstrated in the seminal work of MacDonnell and co-workers, enabled the accumulation of more than two electrons within a single molecular acceptor.[128] The second approach, which has not been yet applied to POM systems, involves the application of intense irradiation to excite simultaneously multiple photosensitizers that are spatially arranged around a central multielectron acceptor and peripheral single-electron donors. Similarly, the use of a pump–pump probe setup (also not explored with POMs systems) allows for the sequential excitation of a unique chromophore generating a doubly excited state.[129,130] The challenges when dealing with charge photo-accumulation is that, once partially reduced, the electron reservoir can potentially promote new energy-wasting pathways that compete with the electron accumulation process. A simplified illustration of the charge accumulation pathway for a POM–PS dyad in the presence of a SED is depicted in Fig. 8. For sake of simplicity, here we consider the SED as an ideal single electron donor (which is rarely the case). Furthermore, we do not consider the reductive quenching of the excited chromophore by the SED but only the oxidation of the SED by PS^+ in the charge-separated state. Ideally, the accumulation of two electrons in the POM proceeds through two light-induced charge separation steps. While the first reduction usually occurs efficiently, the second reduction is slower as reduced POMs, (which behave as electron donor and exhibits visible-light absorption) may undesirably quench the excited PS through reverse charge transfer (blue arrow in Fig. 8) or energy transfer (green arrow in Fig. 8). In general, the design requires a PS with sufficient reducing power to drive several electron transfers to the POM acceptor. In addition, it should also favour a faster accumulative pathway compared to the energy-wasting pathways and the spontaneous reoxidation of the POM, to ensure high yield of the accumulated reducing equivalents.

Our group has reported light-driven charge accumulation using the Wells–Dawson-type POM–heteroleptic Ir(III) assembly described above.[26] In this hybrid, the excited Ir(III) PS has sufficient reducing power ($E(PS^+/PS^*) = -1.36$ V *vs.* SCE) to drive the two-electron reduction of the Dawson polyoxotungstate unit ($\Delta G_1^0 \approx -0.67$ eV and $\Delta G_2^0 \approx -0.22$ eV for the first and second POM reduction). Irradiation of the Dawson hybrid under visible light ($\lambda > 400$ nm) in DMF in the presence of triethylamine (TEA) as SED led to the stepwise reduction of the POM unit. Rapid formation of the one-electron reduced species (1000 W Xe lamp, $\tau_{1/2} = 43$ s, $\tau_{1/2}$ being the time constant, $\phi = 10.5\%$) was followed by a slower formation of the two-electron reduced species ($\tau_{1/2} = 270$ s, $\phi = 2.3\%$). It was shown that adding acetic acid (AcOH) considerably accelerated the rate of the formation of the second reduction ($\tau_{1/2} = 60$ s) by promoting PCET for which POMs have

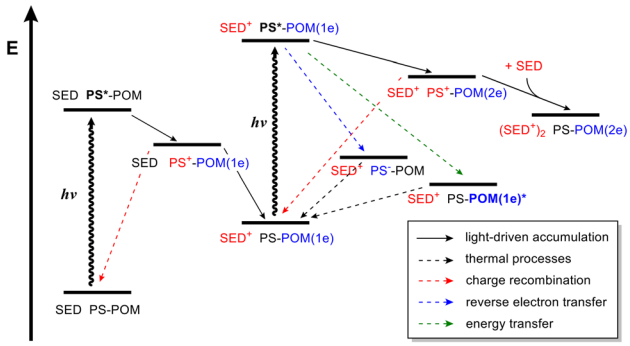

Fig. 8 Pathways and energy diagram of charge photoaccumulation in a POM–PS hybrid dyad in the presence of a one-electron donor SED. Solid arrows represent the light-driven accumulation pathway while the colored dashed arrows represent competing pathways.

strong propensity. The system was also able to produce hydrogen, albeit at low pace, achieving a turnover frequency (TOF) of *ca.* 0.25 h^{-1} and a turnover number (TON) of up to 41 under irradiation for 7 days. Expanding our work on POM–Ir(III) systems, we replaced the picolinate ligand with a less acid labile imidazo-1,10-phenanthroline scaffold and very recently reported the accumulation of up to three electrons in the polyoxomolybdate unit when irradiated in DMF in the presence of TEA and TFA.[31] Meanwhile, no electron was stored in the polyoxotungstate counterpart in which the POM reduction potential is more negative and CS remains ineffective even with acid present. Overall, within these POM–Ir(III) hybrids, the SED is not directly involved in reducing the excited Ir(III)* PS. Instead, the hybrid first undergoes a fast CS, that is, an oxidative quenching of the excited PS by the POM, prior to the regeneration of the PS by the SED.

While often overlooked, the role of the SED is also crucial in the development of charge accumulating systems[131,132] and this was addressed in our very recent work on the POM–bodipy hybrid $[P_2W_{17}O_{61}\{O(SiC_{31}H_{30}N_2BF_2)_2\}]^{6-}$.[110] Several SEDs such as xanthate, triethanolamine, TEA were tested. Yet only TEA (1 M in CH_3CN) promoted the two-electron photo-accumulation in this noble-metal-free hybrid, which completed within 10 min when irradiated with visible light (300 W Xe lamp, $\lambda > 385$ nm) under argon atmosphere. Evaluation of the kinetic profile reveals that the first reduction of the POM is efficient and even improved by acid ($\phi = 11\%$ to 23%). By contrast, the formation of the two-electron reduced POM is much slower ($\phi = 0.6\%$ in the absence of acid), more complex and highly dependent on the strength and quantity of the acid ($\phi = 5.2\%$ in the presence of 20 mM TFA, Fig. 9). The aid of theoretical calculations elucidated an intricate mechanism of the formation of the two-electron reduced species, which is influenced by PCET and acid-promoted POM dismutation. Another pathway involves thermal reduction by the TEA(–H)$^\bullet$ radical, bypassing the photon absorption path, and overall rendering TEA a two-electron, one-proton donor. This study underscores the importance of considering the potential non-innocent role of the SED byproducts and also taking into account how the SED affects the

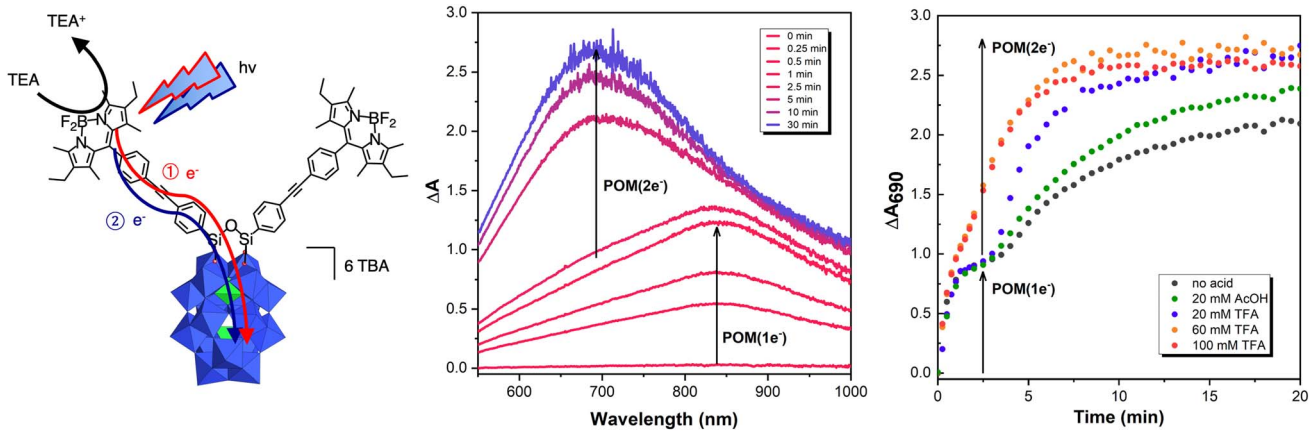

Fig. 9 (Left) Molecular representation of the Dawson–bodipy hybrid. (Middle) Evolution of the absorbance spectra upon irradiation of the hybrid (0.2 mM) in MeCN containing 1 M TEA without acid with 20 mM TFA. (Right) Kinetics of electron accumulation of the hybrid (0.2 mM) in 1 M TEA in MeCN at varying amount of AcOH or TFA monitored at $\lambda_{abs} = 690$ nm. Reproduced and adapted from ref. 107 with permission from the Chinese Chemical Society (CCS) Peking University (PKU), and the Royal Society of Chemistry, copyright 2025.[110]

redox properties of the hybrid POM given that it is often used in large excess (or even as co-solvent).

Charge accumulation was also demonstrated by an unconventional example consisting of a Cu(II)-dipyridylamine complex grafted onto the $\{VO_6\}_3$ cap of a mixed Dawson POM, $[P_2V_3W_{15}O_{62}]^{9-}$.[30] Here, three electrons were successively stored photochemically (one through Cu(II)/Cu(I) reduction, and two through V(V)/V(IV)-centred reductions), although the electron donor remains unidentified. Interestingly, the hybrid was useful in photocatalytically mediating CF_3 radical generation *via* reduction of Togni reagent II, opening avenues to synthetic applications of charge photoaccumulation. By far, non-covalent POM–PS systems exhibiting charge accumulation has been rare. Ishitani and coll., very recently reported a hybrid from the 1 : 1 ion pairing between a cationic ring-shaped Re(I) tetranuclear complex and a Keggin-type POM, ($[XW_{12}O_{40}]^{4-}$ (X = Si, Ge)[29] electron in the ring). Despite the remarkable number of electrons stored, only one or two with sufficient reducing power were supplied to an external catalyst and drive the CO_2 reduction reaction (CO_2RR). Due to the complex composition of most charge accumulation systems, numerous competing pathways that diminish the yield of accumulated reducing equivalents can take place. This may result from side reactions with SED by-products or the inherent reactivity of reduced POMs to traces of oxidants, especially molecular oxygen or oxidizing species formed during the photoirradiation, as we have observed with the POM–bodipy system.[110]

The quenching of the excited PS by reverse electron transfer from the reduced POM (also called 'ping-pong' mechanism)[64,78] is also a limiting issue given that it is a thermodynamically favourable process (Fig. 8). One way to circumvent this is by designing a POM–PS hybrid that possesses rigid molecular bridges and that promotes directional electron transfer (such as in the initial POM–Ir(III) system).[26] Establishing design criteria that improves the stability of photoreduced POM–PS systems and understanding the mechanism of re-oxidation in the dark are some aspects worthy of attention to maximize charge accumulation.

The comparison of the POM–PS compounds displaying charge photoaccumulation properties with other non-POM based systems, in the presence of SEDs, is tedious as the quantum yields of the photoaccumulation are rarely reported.[128,133] In several cases, the efficiency of the overall process were low, probably owing to the presence of aforementioned energy-wasting pathways.[130,134] Yet in one case, a remarkable quantum yield of 66% was reported for the $2e^-$ photoreduction of a Ru(II) complex featuring a fused dipyridophenazine–pyridoquinolinone acceptor ligand.[135] The high efficiency of such system probably relies on the fact that the electron acceptor is involved in the PS* MLCT state that readily react with the SED, a feature that cannot be present in a POM–PS system. Charge photoaccumulation, in the absence of SED, has rarely been reported, and never with a POM acceptor. In most systems featuring a central multielectron acceptor and peripheral PSs, very fast charge separation (below 50 ps) with a low driving force (below 0.5 eV) is observed.[136,137] This characteristic, however, appears challenging to achieve upon electron transfer to POMs owing to the high reorganization energy associated with their polyanionic nature, including solvation effects and counter cations reorganization. Another inspiring strategy, developed by Odobel, Hammarström and coll., relies on the grafting of the molecular system to TiO_2 nanomaterial.[129] Using such an approach, they reported the quantitative formation of a doubly charge separated-state with the oxide materials providing directionality for electron transfer and serving as an electron reservoir.

We have briefly mentioned in the previous examples how the accumulated electrons in the POM can be "released" to drive the reduction of small molecules. Compared to most photocatalytic systems, the most advantageous practical feature of POM–PS is the possibility to temporally decouple photochemical electron storage and thermal re-oxidation in the dark which enables on-demand solar fuel production, like HER. The group of Cronin

and Symes has spurred the application of the decoupling strategy through their pioneering works where they used POMs as mediators to temporally and spatially separate H_2 and O_2 generation in redox flow batteries and water electrolyzers.[138–141] More recently Li, Chen and coll. pursued this approach by incorporating $BiVO_4$ in the system to construct a photoelectrocatalytic system able to decouple H_2 and O_2 evolution in solar-driven water splitting.[142] This concept was also adapted in photochemical POM–PS systems by Streb, Rau, Dietzek and coll. who prepared a hybrid comprising a Ru(II) poylpyridyl complex PS linked to a Dawson polyoxotungstate *via* a phosphonate group.[28] Quantitative accumulation of two electrons was observed after 6 min of irradiation by a monochromatic LED (λ_{max} = 470 nm) in the presence of SEDs such as sodium ascorbate (NaAsc, ϕ = 0.25%) or triethanolamine (TEOA, ϕ = 0.05%). Addition of H_2SO_4 (>10 000 eq.) in the dark triggered instant H_2 generation (up to ~40% yield) and complete re-oxidation of the Ru(II) POM–PS. Remarkably, they were able to store the reduced POM in the dark under inert atmosphere for a long period ($t_{1/2}$ >24 h) and further showed acid-induced H_2 release after 2.5 h storage albeit at a reduced yield (33%) due to partial re-oxidation from an unknown background process.

Since the area of POM–PS photoaccumulation systems is still under development, there is insufficient understanding of reactivity once reducing equivalents are accumulated in the POM, although most systems have been geared towards HER. To understand the "release" of the stored electrons, we can gain insights from studies of the behavior of reduced POMs (*i.e.*, reduced *via* electrochemical or chemical means) exhibiting electron discharge upon the addition of an organic acid.

Guillemot and coll., recently described the study of electron charge/discharge on hybrid Keggin-type polyoxotungstates featuring tertbutylsilanol function coordinated to oxovanadium (V=O).[143] While electrochemical reduction was facilitated in the presence of TFA by virtue of PCET, no hydrogen production was observed due to the weak reducing potential of the electrochemically generated reduced POM species. Chemical reduction using sodium naphthalenide in THF, in contrast, allowed the isolation and characterization of the different reduced forms of the parent POM. One equivalent of the reductant leads to the reduction of the V(V) center to V(IV), while the second equivalent reduces the polyoxotungstic framework leading to a bireduced species possessing decoupled d^1-V(IV) and d^1-W(V). Addition of lutidinium triflate as proton source to the latter resulted in the release of H_2 and the formation of a mono-reduced, monoprotonated species. The same chemical reduction carried out on the same POM without the oxovanadium confirmed that hydrogen evolution takes place at the reduced polyoxotungstic framework. In this system, it was proposed that proton-driven disproportionation of the bireduced species enables the release of hydrogen.

More recently, Matson and coll., also reported spontaneous HER by release of electrons from a chemically mono-reduced $[PW_{12}O_{40}]^{3-}$ in the presence of stoichiometric amounts of a strong organic acid, diphenylammonium ($H_2NPh_2^+$).[18] However, as the monoreduced, monoprotonated species is unstable, it cannot be isolated and characterized. They argued that the ability of this POM to produce H_2 is related to the bond dissociation free energy (BDFE) of the O–H bond on the reduced-protonated species which they estimated from the pK_a and the standard redox potential, E°, of $[PW_{12}O_{40}]^{3-}$ as described by the Bordwell equation (see below), where C_g is a constant associated to proton reduction in the given solvent.[144–146] The study confirms that the BDFE(O–H) of monoreduced, monoprotonated $[PW_{12}O_{40}]^{3-}$ is comparable to that of H_2 BDFE(H–H) in acetonitrile (approx. 50 kcal mol^{-1}) which implies that hydrogen release is thermodynamically favored.

$$\text{BDFE (X–H)} = 1.37\text{p}K_a + 23.06E^\circ + C_g$$

Extending this BDFE-guided study, the same team look at the effect of substituting a W- or P-atom in $[PW_{12}O_{40}]^{3-}$ by a V(V) resulting to $[PVW_{11}O_{40}]^{4-}$ and $[VW_{12}O_{40}]^{3-}$, respectively.[147] The presence of a vanadium dopant positively shifted the first redox potential in both complexes. The presence of V atom at the surface in $[PVW_{11}O_{40}]^{4-}$ also increases its basicity and therefore its affinity for hydrogen atoms. The combined factors ultimately gave rise to higher BDFE (O–H): 68 kcal mol^{-1} in $[PVW_{11}O_{40}]^{4-}$ *vs.* 48 kcal mol^{-1} in $[PW_{12}O_{40}]^{3-}$. Conversely, the presence of an internal V atom dopant in $[VW_{12}O_{40}]^{3-}$ does not affect the surface basicity compared to $[PW_{12}O_{40}]^{3-}$. As a result, HER is less favorable in both cases. The same pattern is observed for vanadium-substituted Lindqvist-type polyoxotungstate, leading to a stable mono reduced monoprotonated species with BDFE(O–H) of 64 kcal mol^{-1}.[148] Overall, this shows that BDFE is a useful metric for predicting a POM's ability to facilitate HER or H-atom transfer, and can guide the design of more effective POMs that can be adapted in hybrid systems.

Although self-evident, it is often overlooked that the reactivity of reduced POMs is ultimately governed not only by the number, but also importantly the reducing strength of the stored electrons. It should be pointed out that while protons facilitate charge accumulation through PCET, this also simultaneously diminishes the reducing power of the stored electrons. Thus, a finely tuned balance of conditions is necessary. While the preceding examples are not photochemical, they highlight the advantage of spatial and/or temporal decoupling between POM reduction and subsequent proton reduction which is a strategy that can preserve the reducing power while promoting HER or the reduction of other substrates.

5 Outlook and conclusions

In the previous section, we discussed the release of electrons from (photo)reduced POMs. The reactions described are either stochiometric (on demand H_2 evolution) or catalytic (HER),[26,36,77,149] including POMs inserted in metal–organic frameworks for HER or CO_2RR.[16] This photoreductive catalysis is an alternative to the common use of POMs in electrocatalysis.[150] Yet some additional insights into the mechanisms driving the reactivity of reduced POMs (especially pristine POMs) in HER or towards organic substrates is still required.

Other than being catalysts themselves, POMs can also take the role of redox mediators or electron shuttles between the photoactive materials and the relevant catalyst. When the development of photo-redox catalysis comes to the interfacing with transparent (semi)-conductive oxide electrodes as in Photo Electrochemical Cells (PECs) and Dye Sensitized Photo Electrochemical Cells (DSPECs), the redox mediator can turn out to be decisive to spatially extend the CS, retard the electron–hole recombination and eventually improve the catalytic efficiency.[151] Note that the lifetime gain is however at the expense of a loss of the driving force to reduce the catalyst.[152] Indeed, photophysical studies on POM–PS hybrids have shown that electron transfers onto/from POMs were significantly slow when the driving force was low, which could be a limitation in the use of these species as redox active shuttle. Mimicking the Z-scheme of natural photosynthesis, Abe and coll. have used $[SiW_{11}MoO_{40}]^{4-/5-}$ and $[SiW_{11}O_{39}Mn^{III}(H_2O)]^{5-/6-}$ couples as effective redox mediators in a visible light-driven multi-photon water splitting system.[153] The electron shuttle role is akin to that of POMs as charge transport layers in optoelectronic devices, where they improve the charge injection at the electrodes.[154] POMs have indeed been diversely applied to improve the performance of dye-sensitized solar cells,[155] either as redox mediators, photosensitizers, interface modification and catalysts for the counter electrode. A study by Gibson, Fielden and coll. showed how Lindqvist polyoxometalate hybrids, co-assembled with a photosensitizer on the surface of NiO photocathodes, could enhance the photovoltage (V_{OC}) by up to 140%.[156] This was caused by CT from the photoreduced dye to the POM electron acceptor and a positive shift in the NiO valence band edge. Charge lifetime and transient IR measurements confirmed that POMs retard both recombination and electron transfer processes. The approach can lead to significant efficiency gains particularly in systems with poorly matched dye/redox mediator combinations. These improvements, however, were offset by reductions in short-circuit current density (J_{SC}). Nonetheless, the approach, if well engineered, could enable regeneration of the PS where there is slow charge-extraction by the redox mediator or catalyst and prevent photodegradation and/or suit applications in photocapacitors.

Biological systems possess self-repairing capabilities that help restore or extend their functions (*e.g.* movement, motility, chemical activity). In natural photosynthesis, for instance, the oxygen-evolving catalyst regenerates approximately every 30 minutes under solar irradiation.[11] In contrast, human-made materials, and particularly those exposed to harsh conditions such as solar flux, degrade over time due to damage induced under operation conditions. Until now, artificial photosynthesis has mostly focused on the performance and robustness of the device. Yet, considering that artificial systems maintained under illumination in aerobic conditions can operate without self-protection is reckless. While the concept of self-healing in artificial photosynthetic device is still in its infancy, supramolecular chemistry with POMs provides tools allowing the elaboration of such materials. For instance, POMs have been integrated in few self-healing gels.[157–159] They also behave as covalently dynamic species in water due to the reversible nature of their structure.[160,161] Such a property was leveraged by Hill, Weinstock and coll. to develop all-inorganic equilibrium systems capable of regenerating the catalytically active species.[162] Similarly, self-repairing properties of hybrid POMs were also reported in case of a reversible anchorage of the organic moieties onto the POM framework.[163] Considering the dynamic nature of the covalent bonds of POMs and the various modes of interactions at work in related materials,[164,165] POMs appear as promising building-blocks for the elaboration of future generation of self-repairing materials for energy applications. Supramolecular chemistry can also be used to control the molecular organization between the polyanionic POM and the organic PS. Typically, controlling molecular organization in photoactive thin films is crucial for enhancing optoelectronic performance.[166,167] For example, the self-assembly of electron donor and acceptor units into highly ordered architectures offers ideal percolation pathways for charge carriers through well-defined nanosegregated D and A domains.[168,169] Furthermore, experimental investigations have shown that D–A systems that assemble into extended architectures can enhance the charge transport properties and considerably prolong the lifetimes of photogenerated excitons.[170] However, creating nanostructured arrays with regularly alternating D and A regions remains challenging due to entropic constraints and the natural tendency of D and A units to stack *via* electronic complementarity, hindering charge transport.[170] A promising approach is to design D–A systems with chemically distinct components to promote effective nanosegregation. As a proof-of-concept, we developed a photoactive mesogenic hybrid POM.[71] In the solid state, the compound, displays a multi-lamellar organization in which double-layers of POMs and the mesogenic organic antenna alternate regularly. Preliminary studies on a next generation of photoactive mesogenic systems showed that such materials display in the solid-state charge-separated states with very long-lived character.[171] Considering the importance of CT processes, such self-assembled materials displaying large D–A interfaces and directional hole/electron transporting pathways could have important impact to further guide the design of optoelectronics materials.

Charge photo-accumulation potentially affords more powerful reductants and could favour multi-electronic reduction processes. However, its scope is much more limited than electrochemically driven electron storage and may be hindered by the reverse electron transfer from the reduced POM to the excited photosensitizer.[78,110] The use of chromophores displaying polarized excited state, such as in heteroleptic metal complexes[51] or in push–pull organic dyes[172–174] can provide directionality to the photoinduced electron transfer, and hence preclude the undesired reverse electron transfer. While electron photoaccumulation has been reported several times on POM–PS the mechanism is not fully understood, especially as these studies required the use of SED, which can be non-innocent in the electron accumulation mechanism. Important effort should be devoted now to perform reversible multi-photon induced charge accumulation in the absence of SEDs.[127] To this end, hybrids associating POMs to multiple photosensitizers are potentially prone to display such multiple charge-separated

states using intense laser excitation energy, as observed by pioneering works of Wasielewski and coll.[136] Typically as many POMs feature bielectronic reduction waves in the presence of an acid source, potential inversion may favour the second reduction of the central core and may lead to long-lived multiple charge separated states, as reported by Wenger and coll.[175] While some information is now accessible on monoelectronic photoinduced electron transfers in POM–PS hybrids, it seems of prime importance to evaluate the kinetics of CS/CR of multiple excited states, and study the effect of the POM protonation in these systems. Understanding the recombination mechanisms of multicharged POM–PS species is of critical importance for carrying out multielectron photoredox catalysis. Another way of performing electron photoaccumulation in the absence of a SED would be to graft the POM–PS species onto a semiconductor (NiO) that would act as an electron pool, inspired by the system developed by Odobel, Hammaström and coll.[129] However, in such a device, protonation is also expected to influence the semiconductor Fermi level by modifying the band edges, which in turn could impact charge transfer at the electrode/PS interface. For NiO, a relatively large driving force for charge separation is required (>0.6 eV), whereas for TiO_2 only *ca.* 0.1–0.2 eV is sufficient.[176] The local environment must also be taken into account (*e.g.*, screening effects, supporting electrolyte, salts, and solvent). In the case of polyanionic species such as POMs, where redox processes are coupled to cation motion and local dielectric, charge stabilization is hindered if ions cannot reorganize rapidly. In solid films or at electrode surfaces, limited ion mobility or the presence of unfavourable counterions could therefore restrict charge accumulation.[177]

The implementation of POM-based photocathodes is thus highly desired, the photoactive materials could be either a molecular photosensitizer or the semi-conducting material (*e.g.* Cu_2O, CIGS). Dye-sensitized photocathodes are a promising approach for converting sunlight into chemical fuels such as H_2 or CO.[178–180] They are often paired with photoanodes (*e.g.*, $BiVO_4$ or dye-sensitized TiO_2) in tandem PECs. In a solar cell, a reversible redox mediator completes the circuit by shuttling charge between the two photoelectrodes.[176,181] In fuel forming PECs, the photoanode oxidizes water, while the photocathode reduces protons to hydrogen or CO_2 to fuels, enabling overall solar-driven water splitting or CO_2 reduction. The fuel forming photocathodes typically consist of a p-type semiconductor (commonly nanostructured NiO) coated with a light-absorbing dye and a molecular catalyst. Suitable dye features have been recently reviewed.[182–184] Device performance is tuned by adjusting dye structure, catalyst properties, and the nanostructure of the semiconductor to balance light absorption, CS, and catalytic activity. Despite much interest, challenges arise due to fast recombination between the reduced dye and oxidized NiO, which limits efficiency. Strategies such as using redox mediators, optimizing dye/catalyst arrangement, and developing new materials are being pursued to address this. As a proof of principle, we demonstrated that Keggin-type POM hybrids co-grafted with a push–pull dye onto nano-ITO cathodes have an amplification effect on the photocurrent response.[179] By anchoring POMs with carboxylic or diazonium groups onto the electrode surface, we achieved controlled POM loading and improved stability against leaching. Remarkably, even at low loading, the POM–COOH hybrid increased the photocurrent response by up to 25 times. It was found that the anchoring group not only stabilized the POM on the electrode but also influenced the complex interplay of electron transfer processes, ultimately boosting photoelectrochemical efficiency. Besides, we observed that the POM presence increased the endurance of the photocathode. Similarly, in the solution state, it was shown that $[Ru(bpy)_3]^{2+}$ exhibited marked photostability when associated with a Wells–Dawson type POM.[33]

To date, covalently bound POM–PS hybrids have not been applied directly in photocathodes, despite many of the photosensitizers used having been integrated in solar cells or fuel forming PECs.[185] Bodipy dyes,[186] for example, can be anchored to metal oxide surfaces (such as TiO_2 or NiO) either *via* traditional carboxylate groups, directly through the boron center or chelating nitrogens, resulting in robust attachment and efficient charge injection.[187] The natural next step would be to develop POM-based photocathodes and, by coupling the dye with suitable molecular catalysts, to see whether the kinetics can be modified, using the molecular systems described above. The flexibility of POM–bodipy hybrids would allow optimization of energy level alignment at the NiO and catalyst interfaces for efficient charge injection and transfer, which is key for photocathode performance. The length, position and conjugation of the spacer between the photosensitizer and anchoring group can be tuned to compromise between fast injection and slow recombination.

Challenges for the integration of hybrid POMs into efficient photocathodes may arise in ensuring good solubility, limiting aggregation on the surface, and good electronic communication through the molecules to the metal oxide. This will be even more challenging when considering the use of aqueous electrolyte (and hence evaluate the stability of the resulting assemblies according to the pH of the solution) and the integration of the catalyst. It will be necessary to test the impacts of structural modifications, electronic coupling and spatial separation between the components, and the environment (electrolyte ions, solvent and pH, for example) on light absorption, photophysics, robustness and catalytic turnover. Therefore, a multidisciplinary approach is needed. However, POM–PS hybrids represent robust, versatile and powerful platforms for advancing the efficiency and functionality of DSPECs for both solar electricity and solar fuel production. Note that a significant step toward practical devices independent of dye design was made by Ryu and coll., who reported a rare example of a POM-based PEC for bias-free solar water splitting. It uses visible-light-active Cu_2O and $BiVO_4$ electrodes, functionalized with TMS-POM catalysts and assembled *via* the Layer-by-Layer technique.[188]

Finally, the use of reduced POMs photosensitivity has emerged as an additional asset for visible-light conversion. Following a series of reports on the visible-light driven reduction of CO_2 to CO over an association of chemically- or electrochemically-reduced $H_3PW_{12}O_{40}$ and rhenium(I) pyridyl–carbonyl complexes and supported by computational studies, the multiple role of the POM has been deciphered and fully

exploited by Neumann and coll. A dispersion of graphitic carbon nitride g-C_3N_4 loaded with the POM and a rhenium catalyst was irradiated with a white LED for a Z-scheme like biphotonic excitation. Photocatalytic hydrocarbon dehydrogenation at the carbon nitride (blue light) was coupled to an electron transfer to the POM and to a subsequent photo-induced electron transfer from the POM to the Re(I) catalyst, by excitation of the intervalence charge transfer band (IVCT) of the bi-reduced POM (red light).[189] In a related example, HER triggered by visible-light induced electron transfer from a reduced form of the Wells–Dawson $[P_2W_{18}O_{62}]^{6-}$ to a cobalt catalyst was described by Duan.[190] This still largely unexplored photosensitization of POMs, which has also found recent applications in photothermal therapy[191] or photothermal catalysis,[192,193] provides a new tool to increase the POM reducing power, and creates a need for insights in the photophysics of reduced POMs.

The POM family offers a full set of tuneable physicochemical properties to devise POM-based photocathodes and DSPECs with improved efficiency and durability for solar energy conversion and multi-electronic processes. One challenge is to make the electron transfer cascade timescales compatible with the fast kinetics of photocathodes, especially those using NiO as a p-type semi-conductor. Furthermore, a robust trapping layer incorporating POMs could be of interest for the photoprotection of molecular photoelectrodes where photodegradation is often attributed to a slow charge extraction, leading to the presence of instable radicals in the materials.[194] Integration of POM-based materials into real device configuration will thus rely on a compromise between synthetic complexity and photophysical performance.

Author contributions

All authors contributed to the writing of the manuscript.

Conflicts of interest

There are no conflicts to declare.

Data availability

This perspective does not contain any original data. All the data presented in this perspective have been sourced from publicly available research studies and data published in peer-reviewed journals.

Acknowledgements

C. C. and L. K./B. acknowledge the Ministère de l'Enseignement Supérieur et de la Recherche (MESR, France) for their PhD fellowship.

Notes and references

1 G. Segev, J. Kibsgaard, C. Hahn, Z. J. Xu, W.-H. Cheng, T. G. Deutsch, C. Xiang, J. Z. Zhang, L. Hammarström, D. G. Nocera, A. Z. Weber, P. Agbo, T. Hisatomi, F. E. Osterloh, K. Domen, F. F. Abdi, S. Haussener, D. J. Miller, S. Ardo, P. C. McIntyre, T. Hannappel, S. Hu, H. Atwater, J. M. Gregoire, M. Z. Ertem, I. D. Sharp, K.-S. Choi, J. S. Lee, O. Ishitani, J. W. Ager, R. R. Prabhakar, A. T. Bell, S. W. Boettcher, K. Vincent, K. Takanabe, V. Artero, R. Napier, B. R. Cuenya, M. T. M. Koper, R. Van De Krol and F. Houle, The 2022 solar fuels roadmap, *J. Phys. Appl. Phys.*, 2022, **55**, 323003.

2 D. Kang, J. L. Young, H. Lim, W. E. Klein, H. Chen, Y. Xi, B. Gai, T. G. Deutsch and J. Yoon, Printed assemblies of GaAs photoelectrodes with decoupled optical and reactive interfaces for unassisted solar water splitting, *Nat. Energy*, 2017, **2**, 17043.

3 W.-H. Cheng, M. H. Richter, M. M. May, J. Ohlmann, D. Lackner, F. Dimroth, T. Hannappel, H. A. Atwater and H.-J. Lewerenz, Monolithic Photoelectrochemical Device for Direct Water Splitting with 19% Efficiency, *ACS Energy Lett.*, 2018, **3**, 1795–1800.

4 Y. Wang, J. Schwartz, J. Gim, R. Hovden and Z. Mi, Stable Unassisted Solar Water Splitting on Semiconductor Photocathodes Protected by Multifunctional GaN Nanostructures, *ACS Energy Lett.*, 2019, **4**, 1541–1548.

5 W.-H. Cheng, M. H. Richter, I. Sullivan, D. M. Larson, C. Xiang, B. S. Brunschwig and H. A. Atwater, CO_2 Reduction to CO with 19% Efficiency in a Solar-Driven Gas Diffusion Electrode Flow Cell under Outdoor Solar Illumination, *ACS Energy Lett.*, 2020, **5**, 470–476.

6 S. Vanka, B. Zhou, R. A. Awni, Z. Song, F. A. Chowdhury, X. Liu, H. Hajibabaei, W. Shi, Y. Xiao, I. A. Navid, A. Pandey, R. Chen, G. A. Botton, T. W. Hamann, D. Wang, Y. Yan and Z. Mi, InGaN/Si Double-Junction Photocathode for Unassisted Solar Water Splitting, *ACS Energy Lett.*, 2020, **5**, 3741–3751.

7 S. K. Karuturi, H. Shen, A. Sharma, F. J. Beck, P. Varadhan, T. Duong, P. R. Narangari, D. Zhang, Y. Wan, J.-H. He, H. H. Tan, C. Jagadish and K. Catchpole, Over 17% Efficiency Stand-Alone Solar Water Splitting Enabled by Perovskite-Silicon Tandem Absorbers, *Adv. Energy Mater.*, 2020, **10**, 2000772.

8 C. Moon, B. Seger, P. C. K. Vesborg, O. Hansen and I. Chorkendorff, Wireless Photoelectrochemical Water Splitting Using Triple-Junction Solar Cell Protected by TiO_2, *Cell Rep. Phys. Sci.*, 2020, **1**, 100261.

9 Y. Wang, A. Sharma, T. Duong, H. Arandiyan, T. Zhao, D. Zhang, Z. Su, M. Garbrecht, F. J. Beck, S. Karuturi, C. Zhao and K. Catchpole, Direct Solar Hydrogen Generation at 20% Efficiency Using Low-Cost Materials, *Adv. Energy Mater.*, 2021, **11**, 2101053.

10 Y. Pihosh, V. Nandal, T. Higashi, R. Shoji, R. Bekarevich, H. Nishiyama, T. Yamada, V. Nicolosi, T. Hisatomi, H. Matsuzaki, K. Seki and K. Domen, Tantalum Nitride-Enabled Solar Water Splitting with Efficiency Above 10%, *Adv. Energy Mater.*, 2023, **13**, 2301327.

11 R. E. Blankenship, *Molecular Mechanisms of Photosynthesis*, Wiley, Chichester, UK, 3rd edn, 2021.

12 N. I. Gumerova and A. Rompel, Synthesis, Structures and Applications of Electron-Rich Polyoxometalates, *Nat. Rev. Chem.*, 2018, **2**, 0112.
13 M. Sadakane and E. Steckhan, Electrochemical properties of polyoxometalates as electrocatalysts, *Chem. Rev.*, 1998, **98**, 219–237.
14 Y. Iwase, O. Tomita, H. Naito, M. Higashi and R. Abe, Molybdenum-substituted polyoxometalate as stable shuttle redox mediator for visible light driven Z-scheme water splitting system, *J. Photochem. Photobiol. Chem.*, 2018, **356**, 347–354.
15 R. Liu, G. Zhang, H. Cao, S. Zhang, Y. Xie, A. Haider, U. Kortz, B. Chen, N. S. Dalal, Y. Zhao, L. Zhi, C.-X. Wu, L.-K. Yan, Z. Su and B. Keita, Enhanced Proton and Electron Reservoir Abilities of Polyoxometalate Grafted on Graphene for High-Performance Hydrogen Evolution, *Energy Environ. Sci.*, 2016, **9**, 1012.
16 N. Li, J. Liu, B. Dong and Y. Lan, Polyoxometalate-Based Compounds for Photo- and Electrocatalytic Applications, *Angew. Chem., Int. Ed.*, 2020, **59**, 20779–20793.
17 M. Girardi, D. Platzer, S. Griveau, F. Bedioui, S. Alves, A. Proust and S. Blanchard, Assessing the Electrocatalytic Properties of the $\{Cp^*Rh^{III}\}^{2+}$-Polyoxometalate Derivative $[H_2PW_{11}O_{39}\{Rh^{III}Cp^*(OH_2)\}]^{3-}$ towards CO_2 Reduction, *Eur. J. Inorg. Chem.*, 2019, **2019**, 387–393.
18 Z. Lu, S. E. Cooney, J. R. McKone and E. M. Matson, Selective Hydrogenation of Azobenzene to Hydrazobenzene via Proton-Coupled Electron Transfer from a Polyoxotungstate Cluster, *JACS Au*, 2024, **4**, 1310–1314.
19 T. Ruther, V. M. Hultgren, B. P. Timko, A. M. Bond, W. R. Jackson and A. G. Wedd, Electrochemical investigation of photooxidation processes promoted by sulfo-polyoxometalates: Coupling of photochemical and electrochemical processes into an effective catalytic cycle, *J. Am. Chem. Soc.*, 2003, **125**, 10133–10143.
20 C. Streb, K. Kastner and J. Tucher, Polyoxometalates in Photocatalysis, *Phys. Sci. Rev.*, 2019, **4**, 20170177.
21 A. J. Kibler, N. Tsang, M. Winslow, S. P. Argent, H. W. Lam, D. Robinson and G. N. Newton, Electronic Structure and Photoactivity of Organoarsenic Hybrid Polyoxometalates, *Inorg. Chem.*, 2023, **62**, 3585–3591.
22 J. J. Walsh, A. M. Bond, R. J. Forster and T. E. Keyes, Hybrid polyoxometalate materials for photo(electro-) chemical applications, *Coord. Chem. Rev.*, 2016, **306**, 217–234.
23 A. Proust, B. Matt, R. Villanneau, G. Guillemot, P. Gouzerh and G. Izzet, Functionalization and post-functionalization: a step towards polyoxometalate-based materials, *Chem. Soc. Rev.*, 2012, **41**, 7605–7622.
24 A. V. Anyushin, A. Kondinski and T. N. Parac-Vogt, Hybrid polyoxometalates as post-functionalization platforms: from fundamentals to emerging applications, *Chem. Soc. Rev.*, 2020, **49**, 382–432.
25 A. Harriman, K. J. Elliott, M. A. H. Alamiry, L. Le Pleux, M. Severac, Y. Pellegrin, E. Blart, C. Fosse, C. Cannizzo, C. R. Mayer and F. Odobel, Intramolecular Electron Transfer Reactions Observed for Dawson-Type Polyoxometalates Covalently Linked to Porphyrin Residues, *J. Phys. Chem. C*, 2009, **113**, 5834–5842.
26 B. Matt, J. Fize, J. Moussa, H. Amouri, A. Pereira, V. Artero, G. Izzet and A. Proust, Charge photo-accumulation and photocatalytic hydrogen evolution under visible light at an iridium(III)-photosensitized polyoxotungstate, *Energy Environ. Sci.*, 2013, **6**, 1504–1508.
27 J. M. Cameron, S. Fujimoto, R.-J. Wei, G. N. Newton and H. Oshio, Post-Functionalization of a Photoactive Hybrid Polyoxotungstate, *Dalton Trans.*, 2018, **47**, 10590–10594.
28 S. Amthor, S. Knoll, M. Heiland, L. Zedler, C. Li, D. Nauroozi, W. Tobaschus, A. K. Mengele, M. Anjass, U. S. Schubert, B. Dietzek-Ivanšić, S. Rau and C. Streb, A Photosensitizer–Polyoxometalate Dyad That Enables the Decoupling of Light and Dark Reactions for Delayed on-Demand Solar Hydrogen Production, *Nat. Chem.*, 2022, **14**, 321–327.
29 M. Takahashi, T. Asatani, T. Morimoto, Y. Kamakura, K. Fujii, M. Yashima, N. Hosokawa, Y. Tamaki and O. Ishitani, Supramolecular Multi-Electron Redox Photosensitisers Comprising a Ring-Shaped Re(I) Tetranuclear Complex and a Polyoxometalate, *Chem. Sci.*, 2023, **14**, 691.
30 W. Wang, L.-M. Chamoreau, G. Izzet, A. Proust, M. Orio and S. Blanchard, Multi-Electron Visible Light Photoaccumulation on a Dipyridylamine Copper(II)–Polyoxometalate Conjugate Applied to Photocatalytic Generation of CF_3 Radicals, *J. Am. Chem. Soc.*, 2023, **145**, 12136–12147.
31 N. Queyriaux, M. Wächtler, C. Cariño, S. Alves, B. Dietzek-Ivanšić, V. Artero, A. Proust, M. Chavarot-Kerlidou and G. Izzet, Covalent POM–Ir hybrid assemblies: tuning redox properties for light-driven multiple charge accumulation, *Chem. Commun.*, 2025, **61**, 9682–9685.
32 R. Ballardini, M. T. Gandolfi and V. Balzani, Dynamic and static quenching of the luminescence of ruthenium(II) polypyridine complexes by heteropolytungstate anions. Direct measurements of intramolecular electron-transfer rate constants, *Inorg. Chem.*, 1987, **26**, 862–867.
33 T. E. Keyes, E. Gicquel, L. Guerin, R. J. Forster, V. Hultgren, A. M. Bond and A. G. Wedd, Photophysical and novel charge-transfer properties of adducts between $[Ru^{II}(bpy)_3]^{2+}$ and $[S_2Mo_{18}O_{62}]^{4-}$, *Inorg. Chem.*, 2003, **42**, 7897–7905.
34 M. K. Seery, N. Fay, T. McCormac, E. Dempsey, R. J. Forster and T. E. Keyes, Photophysics of ruthenium polypyridyl complexes formed with lacunary polyoxotungstates with iron addenda, *Phys. Chem. Chem. Phys.*, 2005, **7**, 3426–3433.
35 N. Fay, V. M. Hultgren, A. G. Wedd, T. E. Keyes, R. J. Forster, D. Leane and A. M. Bond, Sensitization of photo-reduction of the polyoxometalate anions $[S_2M_{18}O_{62}]^{4-}$ (M = Mo, W) in the visible spectral region by the $[Ru(bpy)_3]^{2+}$ cation, *Dalton Trans.*, 2006, 4218–4227.
36 H. Lv, W. Guo, K. Wu, Z. Chen, J. Bacsa, D. G. Musaev, Y. V. Geletii, S. M. Lauinger, T. Lian and C. L. Hill, A Noble-Metal-Free, Tetra-nickel Polyoxotungstate Catalyst

for Efficient Photocatalytic Hydrogen Evolution, *J. Am. Chem. Soc.*, 2014, **136**, 14015–14018.

37 G. Paille, A. Boulmier, A. Bensaid, M.-H. Ha-Thi, T.-T. Tran, T. Pino, J. Marrot, E. Rivière, C. H. Hendon, O. Oms, M. Gomez-Mingot, M. Fontecave, C. Mellot-Draznieks, A. Dolbecq and P. Mialane, An unprecedented $Ni_{14}SiW_9$ hybrid polyoxometalate with high photocatalytic hydrogen evolution activity, *Chem. Commun.*, 2019, **55**, 4166–4169.

38 A. Yokoyama, T. Kojima, K. Ohkubo, M. Shiro and S. Fukuzumi, Formation of a Hybrid Compound Composed of a Saddle-Distorted Tin(IV)—Porphyrin and a Keggin-Type Heteropolyoxometalate To Undergo Intramolecular Photoinduced Electron Transfer, *J. Phys. Chem. A*, 2011, **115**, 986–997.

39 D. Schaming, R. Farha, H. Xu, M. Goldmann and L. Ruhlmann, Formation and Photocatalytic Properties of Nanocomposite Films Containing Both Tetracobalt Dawson-Derived Sandwich Polyanions and Tetracationic Porphyrins, *Langmuir*, 2011, **27**, 132–143.

40 A. Fatima, Y. Smortsova, C. Falaise, N. Leclerc, M. Haouas, E. Cadot, S. Cordier, Y. Molard, T. Pino, C. Dablemont, R. Méallet, K. Steenkeste and M.-H. Ha-Thi, Photoinduced electron transfer between a noble-metal-free $[Mo_6I_8Cl_6]^{2-}$ cluster and polyoxometalates, *Chem. Commun.*, 2023, **59**, 10988–10991.

41 A. W. Maverick, J. S. Najdzionek, D. MacKenzie, D. G. Nocera and H. B. Gray, Spectroscopic, electrochemical, and photochemical properties of molybdenum(II) and tungsten(II) halide clusters, *J. Am. Chem. Soc.*, 1983, **105**, 1878–1882.

42 Z. M. Zhang, T. Zhang, C. Wang, Z. K. Lin, L. S. Long and W. B. Lin, Photosensitizing Metal Organic Framework Enabling Visible-Light-Driven Proton Reduction by a Wells-Dawson-Type Polyoxometalate, *J. Am. Chem. Soc.*, 2015, **137**, 3197–3200.

43 J. Tian, Z.-Y. Xu, D.-W. Zhang, H. Wang, S.-H. Xie, D.-W. Xu, Y.-H. Ren, H. Wang, Y. Liu and Z.-T. Li, Supramolecular metal-organic frameworks that display high homogeneous and heterogeneous photocatalytic activity for H2 production, *Nat. Commun.*, 2016, **7**, 11580.

44 Y. Wang, G. Fang, V. V. Ordomsky and A. Y. Khodakov, Polyoxometalate photocatalysts: solar-driven activation of small molecules for energy conversion and greenhouse gas valorization, *Chem. Commun.*, 2025, **61**, 10630–10642.

45 J. Zhang, M. Zhang, Y. Dong, C. Bai, Y. Feng, L. Jiao and H. Lv, CdTe/CdSe-sensitized photocathode coupling with Ni-substituted polyoxometalate catalyst for photoelectrochemical generation of hydrogen, *Nano Res.*, 2022, **15**, 1347–1354.

46 A. Madonia, M. Martin-Sabi, A. Sadaoui, L. Ruhlmann, S. Ammar and D. Schaming, Dawson-type polyoxometalates photosensitized with carbon dots for photocatalytic reduction of silver ions, *Mater. Res. Bull.*, 2022, **149**, 111721.

47 A. Dolbecq, E. Dumas, C. R. Mayer and P. Mialane, Hybrid Organic-Inorganic Polyoxometalate Compounds: From Structural Diversity to Applications, *Chem. Rev.*, 2010, **110**, 6009–6048.

48 D. Schaming, C. Costa-Coquelard, I. Lampre, S. Sorgues, M. Erard, X. Liu, J. Liu, L. Sun, J. Canny, R. Thouvenot and L. Ruhlmann, Formation of a new hybrid complex via coordination interaction between 5,10,15-tritolyl-20-(4-and 3-pyridyl)porphyrin or 5,10,15-triphenyl-20-(4-pyridyl) porphyrin and the alpha-$[MSiW_{11}O_{39}]^{6-}$ Keggin-type polyoxometalate (M = Co^{2+} and Ni^{2+}), *Inorg. Chim. Acta*, 2010, **363**, 2185–2192.

49 C. Allain, D. Schaming, N. Karakostas, M. Erard, J. P. Gisselbrecht, S. Sorgues, I. Lampre, L. Ruhlmann and B. Hasenknopf, Synthesis, electrochemical and photophysical properties of covalently linked porphyrin-polyoxometalates, *Dalton Trans.*, 2013, **42**, 2745–2754.

50 Y. Luo, M. Wachtler, K. Barthelmes, A. Winter, U. S. Schubert and B. Dietzek, Direct detection of the photoinduced charge-separated state in a Ru(II) bis(terpyridine)polyoxometalate molecular dyad, *Chem. Commun.*, 2018, **54**, 2970–2973.

51 B. Matt, X. Xiang, A. L. Kaledin, N. N. Han, J. Moussa, H. Amouri, S. Alves, C. L. Hill, T. Q. Lian, D. G. Musaev, G. Izzet and A. Proust, Long lived charge separation in iridium(III)-photosensitized polyoxometalates: synthesis, photophysical and computational studies of organometallic-redox tunable oxide assemblies, *Chem. Sci.*, 2013, **4**, 1737–1745.

52 S. Schönweiz, M. Heiland, M. Anjass, T. Jacob, S. Rau and C. Streb, Experimental and Theoretical Investigation of the Light-Driven Hydrogen Evolution by Polyoxometalate–Photosensitizer Dyads, *Chem.–Eur. J.*, 2017, **23**, 15370–15376.

53 F. A. Black, A. Jacquart, G. Toupalas, S. Alves, A. Proust, I. P. Clark, E. A. Gibson and G. Izzet, Rapid photoinduced charge injection into covalent polyoxometalate-bodipy conjugates, *Chem. Sci.*, 2018, **9**, 5578–5584.

54 G. Toupalas, J. Karlsson, F. A. Black, A. Masip-Sanchez, X. Lopez, Y. Ben M'Barek, S. Blanchard, A. Proust, S. Alves, P. Chabera, I. P. Clark, T. Pullerits, J. M. Poblet, E. A. Gibson and G. Izzet, Tuning Photoinduced Electron Transfer in POM-Bodipy Hybrids by Controlling the Environment: Experiment and Theory, *Angew. Chem., Int. Ed.*, 2021, **60**, 6518–6525.

55 M. Choudhari, J. Xu, A. I. McKay, C. Guerrin, C. Forsyth, H. Z. Ma, L. Goerigk, R. A. J. O'Hair, A. Bonnefont, L. Ruhlmann, S. Aloise and C. Ritchie, A photo-switchable molecular capsule: sequential photoinduced processes, *Chem. Sci.*, 2022, **13**, 13732–13740.

56 C. Allain, S. Favette, L. M. Chamoreau, J. Vaissermann, L. Ruhlmann and B. Hasenknopf, Hybrid organic-inorganic porphyrin-polyoxometalate complexes, *Eur. J. Inorg. Chem.*, 2008, 3433–3441.

57 C. Li, N. Mizuno, K. Yamaguchi and K. Suzuki, Self-Assembly of Anionic Polyoxometalate–Organic Architectures Based on Lacunary Phosphomolybdates and Pyridyl Ligands, *J. Am. Chem. Soc.*, 2019, **141**, 7687–7692.

58 M. Bonchio, M. Carraro, G. Scorrano and A. Bagno, Photooxidation in water by new hybrid molecular photocatalysts integrating an organic sensitizer with a polyoxometalate core, *Adv. Synth. Catal.*, 2004, **346**, 648–654.
59 B. B. Xu, M. Lu, J. H. Kang, D. Wang, J. Brown and Z. H. Peng, Synthesis and optical properties of conjugated polymers containing polyoxometalate clusters as side-chain pendants, *Chem. Mater.*, 2005, **17**, 2841–2851.
60 M. Lu, B. H. Xie, J. H. Kang, F. C. Chen, Y. Yang and Z. H. Peng, Synthesis of main-chain polyoxometalate-containing hybrid polymers and their applications in photovoltaic cells, *Chem. Mater.*, 2005, **17**, 402–408.
61 S. Chakraborty, A. Keightley, V. Dusevich, Y. Wang and Z. H. Peng, Synthesis and Optical Properties of a Rod-Coil Diblock Copolymer with Polyoxometalate Clusters Covalently Attached to the Coil Block, *Chem. Mater.*, 2010, **22**, 3995–4006.
62 Y. Li, K. Shetye, K. Baral, L. Jin, J. D. Oster, D.-M. Zhu and Z. Peng, Main-chain polyoxometalate-containing donor–acceptor conjugated copolymers: synthesis, characterization, morphological studies and applications in single-component photovoltaic cells, *RSC Adv.*, 2016, **6**, 29909–29919.
63 F. Odobel, M. Severac, Y. Pellegrin, E. Blart, C. Fosse, C. Cannizzo, C. R. Mayer, K. J. Eliott and A. Harriman, Coupled Sensitizer-Catalyst Dyads: Electron-Transfer Reactions in a Perylene-Polyoxometalate Conjugate, *Chem.–Eur. J.*, 2009, **15**, 3130–3138.
64 K. J. Elliott, A. Harriman, L. Le Pleux, Y. Pellegrin, E. Blart, C. R. Mayer and F. Odobel, A porphyrin-polyoxometallate bio-inspired mimic for artificial photosynthesis, *Phys. Chem. Chem. Phys.*, 2009, **11**, 8767–8773.
65 B. Matt, C. Coudret, C. Viala, D. Jouvenot, F. Loiseau, G. Izzet and A. Proust, Elaboration of Covalently Linked Polyoxometalates with Ruthenium and Pyrene Chromophores and Characteriation of Their Photophysical Properties, *Inorg. Chem.*, 2011, **50**, 7761–7768.
66 B. Matt, J. Moussa, L. M. Chamoreau, C. Afonso, A. Proust, H. Amouri and G. Izzet, Elegant Approach to the Synthesis of a Unique Heteroleptic Cyclometalated Iridium(III)-Polyoxometalate Conjugate, *Organometallics*, 2012, **31**, 35–38.
67 C. Bosch-Navarro, B. Matt, G. Izzet, C. Romero-Nieto, K. Dirian, A. Raya, S. I. Molina, A. Proust, D. M. Guldi, C. Marti-Gastaldo and E. Coronado, Charge transfer interactions in self-assembled single walled carbon nanotubes/Dawson-Wells polyoxometalate hybrids, *Chem. Sci.*, 2014, **5**, 4346–4354.
68 E. Benazzi, J. Karlsson, Y. Ben M'Barek, P. Chabera, S. Blanchard, S. Alves, A. Proust, T. Pullerits, G. Izzet and E. A. Gibson, Acid-triggering of light-induced charge-separation in hybrid organic/inorganic molecular photoactive dyads for harnessing solar energy, *Inorg. Chem. Front.*, 2021, **8**, 1610–1618.
69 Z. Huo, Y. Liang, S. Yang, D. Zang, R. Farha, M. Goldmann, H. Xu, B. Antoine, E. Matricardi, G. Izzet, A. Proust and L. Ruhlmann, Photocurrent generation from visible light irradiation of covalent polyoxometalate–porphyrin copolymers, *Electrochim. Acta*, 2021, **368**, 137635.
70 Z. Huo, B. Akhsassi, J. Yu, M. Zheng, T. Lan, Q. He, C. Boudon, G. Xu, A. Proust, G. Izzet and L. Ruhlmann, Photocatalytic Recovery of Noble Metals by Covalent Silyl Polyoxophosphotungstate–Porphyrin Copolymers, *Inorg. Chem.*, 2025, **64**, 3371–3383.
71 X. Zhu, C. Hessin, A. Salame, L. Sosa-Vargas, D. Kreher, C. Adachi, A. Proust, P. Mialane, J. Marrot, A. Bouchet, M. Sliwa, S. Mery, B. Heinrich, F. Mathevet and G. Izzet, Photoactive Organic/Inorganic Hybrid Materials with Nanosegregated Donor-Acceptor Arrays, *Angew. Chem., Int. Ed.*, 2021, **60**, 8419–8424.
72 I. Azcarate, I. Ahmed, R. Farha, M. Goldmann, X. Wang, H. Xu, B. Hasenknopf, E. Lacôte and L. Ruhlmann, Synthesis and Characterization of Conjugated Dawson-Type Polyoxometalate–Porphyrin Copolymers, *Dalton Trans.*, 2013, **42**, 12688.
73 I. Ahmed, R. Farha, Z. Huo, C. Allain, X. Wang, H. Xu, M. Goldmann, B. Hasenknopf and L. Ruhlmann, Porphyrin–polyoxometalate hybrids connected via a Tris-alkoxo linker for the generation of photocurrent, *Electrochim. Acta*, 2013, **110**, 726–734.
74 Z. H. Huo, D. J. Zang, S. Yang, R. Farha, M. Goldmann, B. Hasenknopf, H. L. Xu and L. Ruhlmann, Synthesis and characterization of Lindqvist-type polyoxometalate-porphyrin copolymers, *Electrochim. Acta*, 2015, **179**, 326–335.
75 M. P. Santoni, A. K. Pal, G. S. Hanan, A. Proust and B. Hasenknopf, Discrete Covalent Organic-Inorganic Hybrids: Terpyridine Functionalized Polyoxometalates Obtained by a Modular Strategy and Their Metal Complexation, *Inorg. Chem.*, 2011, **50**, 6737–6745.
76 T. Auvray, M.-P. Santoni, B. Hasenknopf and G. S. Hanan, Covalent hybrids based on Re(i) tricarbonyl complexes and polypyridine-functionalized polyoxometalate: synthesis, characterization and electronic properties, *Dalton Trans.*, 2017, **46**, 10029–10036.
77 S. Schönweiz, S. A. Rommel, J. Kübel, M. Micheel, B. Dietzek, S. Rau and C. Streb, Covalent Photosensitizer–Polyoxometalate-Catalyst Dyads for Visible-Light-Driven Hydrogen Evolution, *Chem.–Eur. J.*, 2016, **22**, 12002–12005.
78 Y. Luo, S. Maloul, M. Wächtler, A. Winter, U. S. Schubert, C. Streb and B. Dietzek, Is electron ping-pong limiting the catalytic hydrogen evolution activity in covalent photosensitizer–polyoxometalate dyads?, *Chem. Commun.*, 2020, **56**, 10485–10488.
79 Y. Luo, S. Maloul, S. Schonweiz, M. Wachtler, C. Streb and B. Dietzek, Yield-not only Lifetime-of the Photoinduced Charge-Separated State in Iridium Complex-Polyoxometalate Dyads Impact Their Hydrogen Evolution Reactivity, *Chem.–Eur. J.*, 2020, **26**, 8045–8052.
80 Y. Luo, S. Maloul, P. Endres, S. Schönweiz, C. Ritchie, M. Wächtler, A. Winter, U. S. Schubert, C. Streb and

B. Dietzek, Organic linkage controls the photophysical properties of covalent photosensitizer–polyoxometalate hydrogen evolution dyads, *Sustain. Energy Fuels*, 2020, **4**, 4688–4693.

81 C. Rinfray, G. Izzet, J. Pinson, S. G. Derouich, J. J. Ganem, C. Combellas, F. Kanoufi and A. Proust, Electrografting of Diazonium-Functionalized Polyoxometalates: Synthesis, Immobilisation and Electron-Transfer Characterisation from Glassy Carbon, *Chem.–Eur. J.*, 2013, **19**, 13838–13846.

82 K. Barthelmes, M. Sittig, A. Winter and U. S. Schubert, Molecular Dyads and Triads Based on Phenothiazine and π-Extended Tetrathiafulvalene Donors, Bis(terpyridine) ruthenium(II) Complexes, and Polyoxometalates, *Eur. J. Inorg. Chem.*, 2017, **2017**, 3698–3706.

83 Y. S. Luo, M. Wachtler, K. Barthelmes, A. Winter, U. S. Schubert and B. Dietzek, Coexistence of distinct intramolecular electron transfer pathways in polyoxometalate based molecular triads, *Phys. Chem. Chem. Phys.*, 2018, **20**, 11740–11748.

84 K. Suzuki, N. Mizuno and K. Yamaguchi, Polyoxometalate Photocatalysis for Liquid-Phase Selective Organic Functional Group Transformations, *ACS Catal.*, 2018, **8**, 10809–10825.

85 A. Seliverstov and C. Streb, A New Class of Homogeneous Visible-Light Photocatalysts: Molecular Cerium Vanadium Oxide Clusters, *Chem.–Eur. J.*, 2014, **20**, 9733–9738.

86 C. C. Zhao, Z. Q. Huang, W. Rodriguez-Cordoba, C. S. Kambara, K. P. O'Halloran, K. I. Hardcastle, D. G. Musaev, T. Q. Lian and C. L. Hill, Synthesis and Characterization of a Metal-to-Polyoxometalate Charge Transfer Molecular Chromophore, *J. Am. Chem. Soc.*, 2011, **133**, 20134–20137.

87 E. N. Glass, J. Fielden, A. L. Kaledin, D. G. Musaev, T. Lian and C. L. Hill, Extending Metal-to-Polyoxometalate Charge Transfer Lifetimes: The Effect of Heterometal Location, *Chem.–Eur. J.*, 2014, **20**, 4297–4307.

88 J. M. Cameron, S. Fujimoto, K. Kastner, R. J. Wei, D. Robinson, V. Sans, G. N. Newton and H. H. Oshio, Orbital Engineering: Photoactivation of an Organofunctionalized Polyoxotungstate, *Chem.–Eur. J.*, 2017, **23**, 47–50.

89 J. Tucher, K. Peuntinger, J. T. Margraf, T. Clark, D. M. Guldi and C. Streb, Template-Dependent Photochemical Reactivity of Molecular Metal Oxides, *Chem.–Eur. J.*, 2015, **21**, 8716–8719.

90 C. Zhao, W. Rodríguez-Córdoba, A. L. Kaledin, Y. Yang, Y. V. Geletii, T. Lian, D. G. Musaev and C. L. Hill, An Inorganic Chromophore Based on a Molecular Oxide Supported Metal Carbonyl Cluster: $[P_2W_{17}O_{61}\{Re(CO)_3\}_3\{ORb(H_2O)\}(\mu_3\text{-}OH)]^{9-}$, *Inorg. Chem.*, 2013, **52**, 13490–13495.

91 K. Suzuki, F. Tang, Y. Kikukawa, K. Yamaguchi and N. Mizuno, Visible-Light-Induced Photoredox Catalysis with a Tetracerium-Containing Silicotungstate, *Angew. Chem., Int. Ed.*, 2014, **53**, 5356–5360.

92 S. Fujimoto, J. M. Cameron, R.-J. Wei, K. Kastner, D. Robinson, V. Sans, G. N. Newton and H. Oshio, A Simple Approach to the Visible-Light Photoactivation of Molecular Metal Oxides, *Inorg. Chem.*, 2017, **56**, 12169–12177.

93 N. Tsang, A. J. Kibler, S. P. Argent, H. W. Lam, K. D. Jones and G. N. Newton, Organofunctionalized borotungstate polyoxometalates as tunable photocatalysts for oxidative dimerization of amines, *Chem. Sci.*, 2024, **15**, 14685–14691.

94 A. J. Kibler and G. N. Newton, Tuning the electronic structure of organic–inorganic hybrid polyoxometalates: The crucial role of the covalent linkage, *Polyhedron*, 2018, **154**, 1–20.

95 V. Balzani, Supramolecular Photochemistry, *Tetrahedron*, 1992, **48**, 10443–10514.

96 J. P. Sauvage, J. P. Collin, J. C. Chambron, S. Guillerez, C. Coudret, V. Balzani, F. Barigelletti, L. Decola and L. Flamigni, Ruthenium(Ii) And Osmium(Ii) Bis(Terpyridine) Complexes In Covalently-Linked Multicomponent Systems - Synthesis, Electrochemical-Behavior, Absorption-Spectra, And Photochemical And Photophysical Properties, *Chem. Rev.*, 1994, **94**, 993–1019.

97 G. Izzet, F. Volatron and A. Proust, Tailor-made Covalent Organic-Inorganic Polyoxometalate Hybrids: Versatile Platforms for the Elaboration of Functional Molecular Architectures, *Chem. Rec.*, 2017, **17**, 250–266.

98 A. Parrot, A. Bernard, A. Jacquart, S. A. Serapian, C. Bo, E. Derat, O. Oms, A. Dolbecq, A. Proust, R. Metivier, P. Mialane and G. Izzet, Photochromism and Dual-Color Fluorescence in a Polyoxometalate-Benzospiropyran Molecular Switch, *Angew. Chem., Int. Ed.*, 2017, **56**, 4872–4876.

99 M. Laurans, K. Trinh, K. Dalla Francesca, G. Izzet, S. Alves, E. Derat, V. Humblot, O. Pluchery, D. Vuillaume, S. Lenfant, F. Volatron and A. Proust, Covalent Grafting of Polyoxometalate Hybrids onto Flat Silicon/Silicon Oxide: Insights from POMs Layers on Oxides, *ACS Appl. Mater. Interfaces*, 2020, **12**, 48109–48123.

100 S. K. Petrovskii, V. V. Khistiaeva, A. A. Sizova, V. V. Sizov, A. V. Paderina, I. O. Koshevoy, K. Yu. Monakhov and E. V. Grachova, Hexavanadate–Organogold(I) Hybrid Compounds: Synthesis by the Azide–Alkyne Cycloaddition and Density Functional Theory Study of an Intriguing Electron Density Distribution, *Inorg. Chem.*, 2020, **59**, 16122–16126.

101 F. Yang, G. Kalandia, M. Moors, J. Lorenz, M. Rohdenburg, X.-B. Wang, W. Cao, M. A. Moussawi, D. Volke, R. Hoffmann, J. Warneke, T. N. Parac-Vogt and K. Yu. Monakhov, Ligand Substituent Effects on the Electronic Properties of Lindqvist-Type Polyoxometalate Multi-Level-Switches in the Gas Phase, Solution and on Surfaces, *Adv. Mater. Interfaces*, 2024, **11**, 2400411.

102 J. Zhang, F.-P. Xiao, J. Hao and Y.-G. Wei, The Chemistry of Organoimido Derivatives of Polyoxometalates, *Dalton Trans.*, 2012, **41**, 3599.

103 B. R. Hood, Y. de Coene, A. V. Torre Do Vale Froes, C. F. Jones, P. Beaujean, V. Liégeois, F. MacMillan, B. Champagne, K. Clays and J. Fielden, Electrochemically-Switched 2nd Order Non-Linear Optical Response in an

Arylimido-Polyoxometalate with High Contrast and Cyclability, *Angew. Chem., Int. Ed.*, 2023, **62**, e202215537.

104 H. Wu, T. Zhang, L. Yan and Z. Su, Exploration of charge transfer and absorption spectra of porphyrin–polyoxometalate hybrids to search for high performance sensitizers, *RSC Adv.*, 2015, **5**, 93659–93665.

105 J. Li, I. Huth, L. M. Chamoreau, B. Hasenknopf, E. Lacote, S. Thorimbert and M. Malacria, Insertion of Amides into a Polyoxometalate, *Angew. Chem., Int. Ed.*, 2009, **48**, 2035–2038.

106 S. S. Amin, K. D. Jones, A. J. Kibler, H. A. Damian, J. M. Cameron, K. S. Butler, S. P. Argent, M. Winslow, D. Robinson, N. J. Mitchell, H. W. Lam and G. N. Newton, Diphosphoryl-functionalized Polyoxometalates: Structurally and Electronically Tunable Hybrid Molecular Materials, *Angew. Chem., Int. Ed.*, 2023, **62**, e202302446.

107 P. L. Veya and J. K. Kochi, Structural and Spectral Characterization of Novel Charge-Transfer Salts of Polyoxometalates and the Cationic Ferrocenyl Donor, *J. Organomet. Chem.*, 1995, **488**, C4–C8.

108 P. Le Magueres, S. M. Hubig, S. V. Lindeman, P. Veya and J. K. Kochi, Novel Charge-Transfer Materials via Cocrystallization of Planar Aromatic Donors and Spherical Polyoxometalate Acceptors, *J. Am. Chem. Soc.*, 2000, **122**, 10073–10082.

109 A. Winter, P. Endres, E. Schröter, M. Jäger, H. Görls, C. Neumann, A. Turchanin and U. S. Schubert, Towards Covalent Photosensitizer-Polyoxometalate Dyads-Bipyridyl-Functionalized Polyoxometalates and Their Transition Metal Complexes, *Molecules*, 2019, **24**, 4446.

110 C. Cariño, N. Moussa, S. Blanchard, A. Solé-Daura, A. Proust and G. Izzet, Insights into the intricate charge photoaccumulation in a polyoxometalate–bodipy covalent hybrid, *Inorg. Chem. Front.*, 2025, DOI: 10.1039/D5QI01202C.

111 E. N. Glass, J. Fielden, Z. Huang, X. Xiang, D. G. Musaev, T. Lian and C. L. Hill, Transition Metal Substitution Effects on Metal-to-Polyoxometalate Charge Transfer, *Inorg. Chem.*, 2016, **55**, 4308–4319.

112 R. A. Marcus and N. Sutin, Electron transfers in chemistry and biology, *Biochim. Biophys. Acta, Rev. Bioenerg.*, 1985, **811**, 265–322.

113 R. A. Marcus, Electron transfer reactions in chemistry. Theory and experiment, *Rev. Mod. Phys.*, 1993, **65**, 599.

114 D. Rehm and A. Weller, Kinetics And Mechanics Of Electron Transfer During Fluorescence Quenching In Acetonitrile, *Ber. Bunsenges. Phys. Chem.*, 1969, **73**, 834–839.

115 D. Rehm and A. Weller, Kinetics Of Fluorescence Quenching By Electron And H-Atom Transfer, *Isr. J. Chem.*, 1970, **8**, 259–271.

116 A. Saad, O. Oms, A. Dolbecq, C. Menet, R. Dessapt, H. Serier-Brault, E. Allard, K. Baczko and P. Mialane, A high fatigue resistant, photoswitchable fluorescent spiropyran–polyoxometalate–BODIPY single-molecule, *Chem. Commun.*, 2015, **51**, 16088–16091.

117 S. Cetindere, S. T. Clausing, M. Anjass, Y. Luo, S. Kupfer, B. Dietzek and C. Streb, Covalent Linkage of BODIPY-Photosensitizers to Anderson-Type Polyoxometalates Using CLICK Chemistry, *Chem.–Eur. J.*, 2021, **27**, 17181–17187.

118 R. Bevernaegie, L. Marcelis, A. Moreno-Betancourt, B. Laramee-Milette, G. S. Hanan, F. Loiseau, M. Sliwa and B. Elias, Ultrafast charge transfer excited state dynamics in trifluoromethyl-substituted iridium(iii) complexes, *Phys. Chem. Chem. Phys.*, 2018, **20**, 27256–27260.

119 K. Yonesato, S. Yamazoe, S. Kikkawa, D. Yokogawa, K. Yamaguchi and K. Suzuki, Variable control of the electronic states of a silver nanocluster via protonation/deprotonation of polyoxometalate ligands, *Chem. Sci.*, 2022, **13**, 5557–5561.

120 E. Rossin, M. Bonchio, M. Natali and A. Sartorel, Sequential proton coupled electron transfer events from a tetraruthenium polyoxometalate in photochemical water oxidation, *Sustain. Energy Fuels*, 2024, **8**, 1944–1952.

121 S. Himeno, M. Takamoto, R. Santo and A. Ichimura, Redox properties and basicity of Keggin-type polyoxometalate complexes, *Bull. Chem. Soc. Jpn.*, 2005, **78**, 95–100.

122 S. X. Guo, A. W. A. Mariotti, C. Schlipf, A. M. Bond and A. G. Wedd, A Systematic approach to the simulation of the voltammetric reduction of [alpha-$SiW_{12}O_{40}$]$^{4-}$ in buffered aqueous electrolyte media and acetonitrile, *J. Electroanal. Chem.*, 2006, **591**, 7–18.

123 V. A. Grigoriev, C. L. Hill and I. A. Weinstock, Role of cation size in the energy of electron transfer to 1 : 1 polyoxometalate ion pairs $\{(M^+)(X^{n+}VW_{11}O_{40})\}^{(8n)-}$ (M = Li, Na, K), *J. Am. Chem. Soc.*, 2000, **122**, 3544–3545.

124 B. Keita, D. Bouaziz and L. Nadjo, Solvent Effects on the Redox Potentials of Potassium 12-Tungstosilicate and 18-Tungstodiphosphate, *J. Electrochem. Soc.*, 1988, **135**, 87.

125 Y. Pellegrin and F. Odobel, Molecular devices featuring sequential photoinduced charge separations for the storage of multiple redox equivalents, *Coord. Chem. Rev.*, 2011, **255**, 2578–2593.

126 L. Hammarstrom, Accumulative Charge Separation for Solar Fuels Production: Coupling Light-Induced Single Electron Transfer to Multielectron Catalysis, *Acc. Chem. Res.*, 2015, **48**, 840–850.

127 T. H. Bürgin and O. S. Wenger, Recent Advances and Perspectives in Photodriven Charge Accumulation in Molecular Compounds: A Mini Review, *Energy Fuels*, 2021, **35**, 18848–18856.

128 R. Konduri, H. W. Ye, F. M. MacDonnell, S. Serroni, S. Campagna and K. Rajeshwar, Ruthenium photocatalysts capable of reversibly storing up to four electrons in a single acceptor ligand: A step closer to artificial photosynthesis, *Angew. Chem., Int. Ed.*, 2002, **41**, 3185–3187.

129 S. Karlsson, J. Boixel, Y. Pellegrin, E. Blart, H. C. Becker, F. Odobel and L. Hammarström, Accumulative Charge Separation Inspired by Photosynthesis, *J. Am. Chem. Soc.*, 2010, **132**, 17977–17979.

130 S. Mendes Marinho, M.-H. Ha-Thi, V.-T. Pham, A. Quaranta, T. Pino, C. Lefumeux, T. Chamaillé, W. Leibl and A. Aukauloo, Time-Resolved Interception of Multiple-

Charge Accumulation in a Sensitizer–Acceptor Dyad, *Angew. Chem., Int. Ed.*, 2017, **56**, 15936–15940.
131 Y. Pellegrin and F. Odobel, Sacrificial electron donor reagents for solar fuel production, *Artif. Photosynth.*, 2017, **20**, 283–295.
132 J. C. Bawden, P. S. Francis, S. DiLuzio, D. J. Hayne, E. H. Doeven, J. Truong, R. Alexander, L. C. Henderson, D. E. Gómez, M. Massi, B. I. Armstrong, F. A. Draper, S. Bernhard and T. U. Connell, Reinterpreting the Fate of Iridium(III) Photocatalysts-Screening a Combinatorial Library to Explore Light-Driven Side-Reactions, *J. Am. Chem. Soc.*, 2022, **144**, 11189–11202.
133 J. Nomrowski, X. Guo and O. S. Wenger, Charge Accumulation and Multi-Electron Photoredox Chemistry with a Sensitizer-Catalyst-Sensitizer Triad, *Chem.–Eur. J.*, 2018, **24**, 14084–14087.
134 M. Schulz, N. Hagmeyer, F. Wehmeyer, G. Lowe, M. Rosenkranz, B. Seidler, A. Popov, C. Streb, J. G. Vos and B. Dietzek, Photoinduced Charge Accumulation and Prolonged Multielectron Storage for the Separation of Light and Dark Reaction, *J. Am. Chem. Soc.*, 2020, **142**, 15722–15728.
135 J.-F. Lefebvre, J. Schindler, P. Traber, Y. Zhang, S. Kupfer, S. Gräfe, I. Baussanne, M. Demeunynck, J.-M. Mouesca, S. Gambarelli, V. Artero, B. Dietzek and M. Chavarot-Kerlidou, An Artificial Photosynthetic System for Photoaccumulation of Two Electrons on a Fused Dipyridophenazine (Dppz)–Pyridoquinolinone Ligand, *Chem. Sci.*, 2018, **9**, 4152–4159.
136 M. P. Oneil, M. P. Niemczyk, W. A. Svec, D. Gosztola, G. L. Gaines and M. R. Wasielewski, Picosecond Optical Switching Based On Biphotonic Excitation Of An Electron Donor-Acceptor-Donor Molecule, *Science*, 1992, **257**, 63–65.
137 M. Orazietti, M. Kuss-Petermann, P. Hamm and O. S. Wenger, Light-Driven Electron Accumulation in a Molecular Pentad, *Angew. Chem., Int. Ed.*, 2016, **55**, 9407.
138 M. D. Symes and L. Cronin, Decoupling hydrogen and oxygen evolution during electrolytic water splitting using an electron-coupled-proton buffer, *Nat. Chem.*, 2013, **5**, 403–409.
139 B. Rausch, M. D. Symes, G. Chisholm and L. Cronin, Decoupled catalytic hydrogen evolution from a molecular metal oxide redox mediator in water splitting, *Science*, 2014, **345**, 1326–1330.
140 J. J. Chen, M. D. Symes and L. Cronin, Highly reduced and protonated aqueous solutions of $[P_2W_{18}O_{62}](6-)$ for on-demand hydrogen generation and energy storage, *Nat. Chem.*, 2018, **10**, 1042–1047.
141 O. Mbang Eze, Z. Ertekin and M. D. Symes, Decoupled Water Electrolysis at High Current Densities Using a Solution-Phase Redox Mediator, *Energy Fuels*, 2025, **39**, 7129–7136.
142 L.-P. Cui, S. Zhang, Y. Zhao, X.-Y. Ge, L. Yang, K. Li, L.-B. Feng, R.-G. Li and J.-J. Chen, Tunable multi-electron redox polyoxometalates for decoupled water splitting driven by sunlight, *Nat. Commun.*, 2025, **16**, 3674.
143 L. K/Bidi, A. Desjonquères, G. Izzet and G. Guillemot, H2 Evolution at a Reduced Hybrid Polyoxometalate and Its Vanadium-Oxo Derivative Used as Molecular Models for Reducible Metal Oxides, *Inorg. Chem.*, 2023, **62**, 1935–1941.
144 J. J. Warren, T. A. Tronic and J. M. Mayer, Thermochemistry of Proton-Coupled Electron Transfer Reagents and its Implications, *Chem. Rev.*, 2010, **110**, 6961–7001.
145 C. F. Wise, R. G. Agarwal and J. M. Mayer, Determining Proton-Coupled Standard Potentials and X–H Bond Dissociation Free Energies in Nonaqueous Solvents Using Open-Circuit Potential Measurements, *J. Am. Chem. Soc.*, 2020, **142**, 10681–10691.
146 R. G. Agarwal, S. C. Coste, B. D. Groff, A. M. Heuer, H. Noh, G. A. Parada, C. F. Wise, E. M. Nichols, J. J. Warren and J. M. Mayer, Free Energies of Proton-Coupled Electron Transfer Reagents and Their Applications, *Chem. Rev.*, 2022, **122**, 1–49.
147 Z. Lu, M. Dagar, J. R. McKone and E. M. Matson, Location of dopant dictates proton–coupled electron transfer mechanism in vanadium-substituted polyoxotungstates, *Chem. Sci.*, 2025, **16**, 6736–6743.
148 D. Shiels, Z. Lu, M. Pascual-Borràs, N. Cajiao, T. V. Marinho, W. W. Brennessel, M. L. Neidig, R. J. Errington and E. M. Matson, Vanadium Substitution Dictates H Atom Uptake at Lindqvist-type Polyoxotungstates, *Inorg. Chem.*, 2024, **63**, 23304–23316.
149 M. Zhao, Q. Liu, Y. Feng and H. Lv, Recent advances in polyoxometalate-based catalysts for light-driven hydrogen evolution, *Dalton Trans.*, 2024, **53**, 18083–18088.
150 B. Fabre, C. Falaise and E. Cadot, Polyoxometalates-Functionalized Electrodes for (Photo)Electrocatalytic Applications: Recent Advances and Prospects, *ACS Catal.*, 2022, **12**, 12055–12091.
151 B. Shan, M. K. Brennaman, L. Troian-Gautier, Y. Liu, A. Nayak, C. M. Klug, T.-T. Li, R. M. Bullock and T. J. Meyer, A Silicon-Based Heterojunction Integrated with a Molecular Excited State in a Water-Splitting Tandem Cell, *J. Am. Chem. Soc.*, 2019, **141**, 10390–10398.
152 R. Godin and J. R. Durrant, Dynamics of photoconversion processes: the energetic cost of lifetime gain in photosynthetic and photovoltaic systems, *Chem. Soc. Rev.*, 2021, **50**, 13372–13409.
153 K. Tsuji, O. Tomita, M. Higashi and R. Abe, Manganese-Substituted Polyoxometalate as an Effective Shuttle Redox Mediator in Z-Scheme Water Splitting under Visible Light, *ChemSusChem*, 2016, **9**, 2201–2208.
154 Y. Hu, Y. Wang, J. Zhao and L. Chen, Recent advances of polyoxometalate-based materials applied for electron-related devices, *Coord. Chem. Rev.*, 2024, **506**, 215724.
155 L. Chen, W.-L. Chen, X.-L. Wang, Y.-G. Li, Z.-M. Su and E.-B. Wang, Polyoxometalates in dye-sensitized solar cells, *Chem. Soc. Rev.*, 2019, **48**, 260–284.
156 H. El Moll, F. A. Black, C. J. Wood, A. Al-Yasari, A. Reddy Marri, I. V. Sazanovich, E. A. Gibson and J. Fielden, Increasing P-Type Dye Sensitised Solar Cell Photovoltages Using Polyoxometalates, *Phys. Chem. Chem. Phys.*, 2017, **19**, 18831.

157 J. Yang, M. Chen, P. Li, F. Cheng, Y. Xu, Z. Li, Y. Wang and H. Li, Self-healing hydrogel containing Eu-polyoxometalate as acid-base vapor modulated luminescent switch, *Sens. Actuators, B*, 2018, **273**, 153–158.

158 L. Casimiro, F. Volatron, G. Boivin, B. Abécassis, S. Alves, D. Brouri, D. Montero, J.-M. Guigner, L.-M. Chamoreau, G. Gontard, D. Portehault, Y. Li, A. Proust, R. Lescouëzec, G. Ducouret, A. Solé-Daura, P. Davidson, T. Merland and G. Izzet, Multifunctional Supramolecular Gels with Strong Mechanical Properties Formed by Self-Assembly of Polyoxometalate-Based Coordination Polymers, *JACS Au*, 2024, **4**, 4948–4956.

159 A. Shaheen, P. Kour, U. N. Tak, H. A. Mir, G. Ahanger, S. Sidiq and A. A. Dar, Multifunctional Chitosan–Polyoxometalate-Based Hydrogel Beads for UV Light Detection, Inkless Erasable Printing, Heterogenous Catalysis, and Antibacterial Applications, *ACS Appl. Eng. Mater.*, 2024, **2**, 1706–1723.

160 H. N. Miras, D.-L. Long and L. Cronin, in *Advances in Inorganic Chemistry*, ed. R. van Eldik and L. Cronin, Academic Press, 2017, vol. 69, pp. 1–28.

161 A. Kondinski and M. Ghorbani-Asl, Polyoxoplatinates as covalently dynamic electron sponges and molecular electronics materials, *Nanoscale Adv.*, 2021, **3**, 5663–5675.

162 I. A. Weinstock, E. M. G. Barbuzzi, M. W. Wemple, J. J. Cowan, R. S. Reiner, D. M. Sonnen, R. A. Heintz, J. S. Bond and C. L. Hill, Equilibrating metal-oxide cluster ensembles for oxidation reactions using oxygen in water, *Nature*, 2001, **414**, 191–195.

163 G. Izzet, M. Ménand, B. Matt, S. Renaudineau, L. M. Chamoreau, M. Sollogoub and A. Proust, Cyclodextrin-Induced Auto-Healing of Hybrid Polyoxometalates, *Angew. Chem., Int. Ed.*, 2012, **51**, 487–490.

164 Y. F. Song and R. Tsunashima, Recent advances on polyoxometalate-based molecular and composite materials, *Chem. Soc. Rev.*, 2012, **41**, 7384–7402.

165 J. M. Cameron, G. Guillemot, T. Galambos, S. S. Amin, E. Hampson, K. Mall Haidaraly, G. N. Newton and G. Izzet, Supramolecular assemblies of organo-functionalised hybrid polyoxometalates: from functional building blocks to hierarchical nanomaterials, *Chem. Soc. Rev.*, 2022, **51**, 293–328.

166 A. R. Murphy and J. M. J. Fréchet, Organic semiconducting oligomers for use in thin film transistors, *Chem. Rev.*, 2007, **107**, 1066–1096.

167 H. Iino, T. Usui and J. Hanna, Liquid crystals for organic thin-film transistors, *Nat. Chem.*, 2015, **6**, 6828.

168 P. O. Schwartz, L. Biniek, E. Zaborova, B. Heinrich, M. Brinkmann, N. Leclerc and S. Méry, Perylenediimide-Based Donor-Acceptor Dyads and Triads: Impact of Molecular Architecture on Self-Assembling Properties, *J. Am. Chem. Soc.*, 2014, **136**, 5981–5992.

169 M. Hecht, T. Schlossarek, M. Stolte, M. Lehmann and F. Wurthner, Photoconductive Core-Shell Liquid-Crystal of Perylene Bisimide J-Aggregate Donor-Acceptor Dyad, *Angew. Chem., Int. Ed.*, 2019, **58**, 12979–12983.

170 M. Madhu, R. Ramakrishnan, V. Vijay and M. Hariharan, Free Charge Carriers in Homo-Sorted π-Stacks of Donor–Acceptor Conjugates, *Chem. Rev.*, 2021, **121**, 8234–8284.

171 Unpubl. Results.

172 H. Wang, C. Zhao, Z. Burešová, F. Bureš and J. Liu, Cyano-capped molecules: versatile organic materials, *J. Mater. Chem. A*, 2023, **11**, 3753–3770.

173 A. A. Raheem and C. Praveen, π-Distorted charge transfer chromophores and their materials chemistry in organic photovoltaics, *J. Mater. Chem. C*, 2024, **12**, 8611–8646.

174 K. Xue, X.-Z. Zhu, J.-F. Yan, S.-H. Chen and Y.-F. Yuan, Advances in Nonlinear Optics of Twisted Push Pull Organic Chromophores, *ChemPhotoChem*, 2025, 2500017.

175 J. Nomrowski and O. S. Wenger, Exploiting Potential Inversion for Photoinduced Multielectron Transfer and Accumulation of Redox Equivalents in a Molecular Heptad, *J. Am. Chem. Soc.*, 2018, **140**, 5343–5346.

176 A. B. Muñoz-García, I. Benesperi, G. Boschloo, J. J. Concepcion, J. H. Delcamp, E. A. Gibson, G. J. Meyer, M. Pavone, H. Pettersson, A. Hagfeldt and M. Freitag, Dye-sensitized solar cells strike back, *Chem. Soc. Rev.*, 2021, **50**, 12450–12550.

177 F. Zhao, T. Cheng, X. Lu, N. Ghorai, Y. Yang, Y. V. Geletii, D. G. Musaev, C. L. Hill and T. Lian, Charge Transfer Mechanism on a Cobalt-Polyoxometalate-TiO_2 Photoanode for Water Oxidation in Acid, *J. Am. Chem. Soc.*, 2024, **146**, 14600–14609.

178 E. A. Gibson, Dye-sensitized photocathodes for H_2 evolution, *Chem. Soc. Rev.*, 2017, **46**, 6194–6209.

179 Y. Ben M'Barek, T. Rosser, J. Sum, S. Blanchard, F. Volatron, G. Izzet, R. Salles, J. Fize, M. Koepf, M. Chavarot-Kerlidou, V. Artero and A. Proust, Dye-Sensitized Photocathodes: Boosting Photoelectrochemical Performances with Polyoxometalate Electron Transfer Mediators, *ACS Appl. Energy Mater.*, 2020, **3**, 163–169.

180 K. Zhu, G. Mul and A. Huijser, Dye-sensitized NiO photocathodes: Research progress, current mechanistic understanding, and research perspectives, *Chem. Phys. Rev.*, 2024, **5**, 021305.

181 D. N. Nguyen, E. Giannoudis, T. Straistari, J. Fize, M. Koepf, P. D. Tran, M. Chavarot-Kerlidou and V. Artero, Unassisted Solar Syngas Production by a Molecular Dye-Cobalt Catalyst Assembly in a Tandem Photoelectrochemical Cell, *ACS Energy Lett.*, 2024, **9**, 829–834.

182 I. Heath-Apostolopoulos, D. Vargas-Ortiz, L. Wilbraham, K. E. Jelfs and M. A. Zwijnenburg, Using high-throughput virtual screening to explore the optoelectronic property space of organic dyes; finding diketopyrrolopyrrole dyes for dye-sensitized water splitting and solar cells, *Sustain. Energy Fuels*, 2021, **5**, 704–719.

183 X.-L. Wang, J.-F. Huang, J.-M. Liu and P. Tsiakaras, Recent advances in metal-free photosensitizers for dye-sensitized photoelectrochemical cells, *Coord. Chem. Rev.*, 2025, **522**, 216143.

184 L. Fei, L. Lei, T. J. Meyer and D. Wang, Dye-Sensitized Photocathodes Assembly and Tandem

Photoelectrochemical Cells for CO_2 Reduction, *Acc. Mater. Res.*, 2024, **5**, 124–135.

185 E. Benazzi, J. Mallows, G. H. Summers, F. A. Black and E. A. Gibson, Developing photocathode materials for p-type dye-sensitized solar cells, *J. Mater. Chem. C*, 2019, **7**, 10409–10445.

186 R. D. James, L. S. Alqahtani, J. Mallows, H. V. Flint, P. G. Waddell, O. J. Woodford and E. A. Gibson, Pentafluorosulfanyl-functionalised BODIPY push–pull dyes for p-type dye-sensitized solar cells, *Sustain. Energy Fuels*, 2023, **7**, 1494–1501.

187 H. Klfout, A. Stewart, M. Elkhalifa and H. He, BODIPYs for Dye-Sensitized Solar Cells, *ACS Appl. Mater. Interfaces*, 2017, **9**, 39873–39889.

188 H. Kim, S. Bae, D. Jeon and J. Ryu, Fully solution-processable Cu_2 O–$BiVO_4$ photoelectrochemical cells for bias-free solar water splitting, *Green Chem.*, 2018, **20**, 3732–3742.

189 H. Yu, E. Haviv and R. Neumann, Visible-Light Photochemical Reduction of CO_2 to CO Coupled to Hydrocarbon Dehydrogenation, *Angew. Chem., Int. Ed.*, 2020, **59**, 6219–6223.

190 W. Sun, B. An, B. Qi, T. Liu, M. Jin and C. Duan, Dual-Excitation Polyoxometalate-Based Frameworks for One-Pot Light-Driven Hydrogen Evolution and Oxidative Dehydrogenation, *ACS Appl. Mater. Interfaces*, 2018, **10**, 13462–13469.

191 C. Zhang, W. Bu, D. Ni, C. Zuo, C. Cheng, Q. Li, L. Zhang, Z. Wang and J. Shi, A Polyoxometalate Cluster Paradigm with Self-Adaptive Electronic Structure for Acidity/Reducibility-Specific Photothermal Conversion, *J. Am. Chem. Soc.*, 2016, **138**, 8156–8164.

192 X. Chen, G. Zhang, B. Li and L. Wu, An integrated giant polyoxometalate complex for photothermally enhanced catalytic oxidation, *Sci. Adv.*, 2021, **7**, eabf8413.

193 X. Chen, Q. Li, M. Li, M. Shi, M. Liang, Y. Chen, F. Bai and Y.-Q. Lan, Frontiers in Polyoxometalate-Based Hybrids for Photothermal Catalysis, *Adv. Funct. Mater.*, 2025, e10863.

194 S. Bold, J. Massin, E. Giannoudis, M. Koepf, V. Artero, B. Dietzek and M. Chavarot-Kerlidou, Spectroscopic Investigations Provide a Rationale for the Hydrogen-Evolving Activity of Dye-Sensitized Photocathodes Based on a Cobalt Tetraazamacrocyclic Catalyst, *ACS Catal.*, 2021, **11**, 3662–3678.